European Sovereign Systemic Risk Zones

Veni Arakelian[a], Petros Dellaportas[b], Roberto Savona[c,*], Marika Vezzoli[d]

[a] *Department of Economic and Regional Development, Panteion University, Greece.*
[b] *Department of Statistical Science, University College London, UK.*
[c] *Department of Economics and Management, University of Brescia, Italy.*
[d] *Department of Molecular and Translational Medicine, University of Brescia, Italy.*

Abstract

This paper proposes a novel framework identifying sovereign systemic risk zones. We first explore the cross-dynamics of sovereign CDS in terms of time-changing contagion measures based on copulas. The approach is based on reversible jump MCMC sampling and the daily estimated dependencies are expressed with Bayesian model-averaging estimates of Kendall's τ. These measures are then assembled together with country-specific fundamentals through recursive partitioning, thereby producing important leading indicators and identification of main sovereign systemic risk regimes expressed as regions in CDS spreads. Using data for Greece, Ireland, Italy, Portugal, Spain, France, Germany over the period 2008-2013, we identify three main systemic risk zones (safe, risky, high risky) also assigning specific risk thresholds to the selected leading indicators (unemployment rate, Debt/GDP, inflation, GDP growth, copula-based CDS dependencies).

JEL classification: G12, G01.

Keywords: Credit default swaps, systemic risk, contagion, copula, regression trees.

*Corresponding author
Email addresses: varakelian@panteion.gr (Veni Arakelian), p.dellaportas@ucl.ac.uk (Petros Dellaportas), roberto.savona@unibs.it (Roberto Savona), marika.vezzoli@unibs.it. (Marika Vezzoli)

1. Introduction

Sovereign credit default swap spreads (CDS) were gradually narrowing from April to September 2009 in response to the taxpayer bailout that subsidised the risk. Yet, the deterioration of bank debts resulted in higher levels of sovereign risk from November 2009, shortly after the election of the new Greek government and the revision that more than doubled Greek public sector deficit. On April 26, 2010, three days after the Greek prime minister asked European Union and the International Monetary Fund for financial help, the Greek 5-yr sovereign CDS spread reached the 700 bps and its trading status changed to up front[1], as the protection buyer had to pay a portion of the notional amount insured besides the coupon, implying that the sellers of default protection are demanding a deposit at the inception of the trade to cover the country's deteriorating credit risk. The CDS spread of Italy, Spain, Portugal and Ireland behaved similarly to that of Greece. On August 2010, when the risk of Irish debt was very high, there was also a rising trend in the CDS spread of Greece, Italy, Spain and Portugal. At the end of 2011 and the start of 2012, the CDS spreads of GIIPS soared, with the Greek CDS spread reaching sky high levels before Greece's restructuring in March 2012.

During that period, academics, bankers, regulators and policymakers considered systemic sovereign risk as a novel risk entity. It is now broadly believed that what previously appeared as a homogeneous and safe macro area in terms of sovereign risks, seems in fact to generate regime shifts in credit spreads, with large changes in the eco-financial systems and severe impacts on economies.

[1]According to O' Kane (2008) the trading status of CDS changes then reaching 1000 bps. In the case of the Greek CDS various trading desks changed its status at the 700 bps

Detecting sovereign systemic risk zones is of fundamental financial importance from a public policy perspective. The early detection and causal identification of such phenomena may provide valuable early warning signals to countries moving towards dangerous risk paths. Moreover, it is of primary interest to provide effective risk mapping in which country-specific fundamentals are united with contagion-based measures, thereby assembling a series of leading indicators that could signal impending sovereign systemic risk abnormalities.

The purpose of our study is to identify these regime shifts and provide a sovereign risk stratification that can be identified by country fundamentals and sovereign contagion measures. We explore the relationship between systemic sovereign credit risk for Greece, Ireland, Italy, Portugal and Spain (hereafter GIIPS), France and Germany. We use daily quotes of the 5-yr sovereign CDS spreads and leading macroeconomic country-specific indicators. Additionally we use US sovereign credit risk to examine its impact, as the recent literature indicates the US financial channel as a global source of risk (Longstaff et al. (2011), Augustin and Tedongap (2014)). We complement the literature on sovereign systemic risk through the following modelling scenario: firstly, we explore the cross-dynamics of sovereign CDS spreads in terms of time-changing contagion measures based on copulas. We then assemble these measures together with country-specific fundamentals producing important leading indicators and leading to identification of the main sovereign systemic risk regimes expressed as regions in CDS spreads.

The novelty of our perspective is that we examine whether contagion, expressed as a dependence measure via Kendall's τ, after controlling with specific fundamentals, affects CDS spreads. Such an approach, using a proxy of dependence as a predictor, has never been investigated in the financial literature.

A key aspect of our analysis is that we employ nonparametric statistical modelling tools with inferential procedures based on ensemble learning. Nonparametric modelling is needed when highly complex stochastic systems are analysed, as parametric models fail to deal adequately with the high dimensional nonlinearities presented in the data. Moreover, our statistical inferences are based on ensemble learning, expressed via either Bayesian model averaging or bootstrap aggregating (bagging). We therefore adopt this modern, popular methodology to strengthen inferences by combining a number of statistical models, rather than just one. We measure the contagion between CDS spreads by employing a rich Bayesian model averaging strategy in which various copula specifications that are allowed to change in time produce a nonlinear dependency measurement expressed as a posterior mean of Kendall's τ. The time changing process of copula specifications is based on thresholds which have unknown locations and a-priori unknown numbers. The resulting measures are therefore highly nonlinear, as they are produced as averages across models with different copulas, a different number of thresholds and different threshold locations. Inference is achieved through a population-based, reversible-jump MCMC algorithm. In a second stage, we employ regression trees to detect the most important leading indicators for each country and identify the main sovereign systemic risk regimes. The procedure approximates the sovereign risk dynamics as a union of piecewise linear functions, where observations are grouped through multidimensional data splits. Inference is based on random forests, a bootstrap aggregating ensemble meta-algorithm which has turned out to be a very valuable inference method in regression trees literature when the size of the tree is large.

The statistical analysis provides evidence for three systemic risk zones.The *safe zone* is characterised by a low unemployment rate and moderate Debt/GDP ratio, the *risky*

zone has a high unemployment rate or high Debt/GDP ratio, and the *high risky zone* is characterised by a high unemployment rate, high Debt/GDP ratio and significant sovereign dependency. The novelty of these findings is that for each leading indicator we provide a corresponding risk threshold, also allowing non-linear interactions among them with potentially relevant policy implications. Indeed, an unemployment rate up to 11.75 per cent together with a Debt/GDP ratio up to 119.6 per cent should maintain sovereign spreads within a safe zone. On the other hands, when unemployment rate exceeds 11.75 per cent or Debt/GDP ratio is crossing 119.6 per cent, the sovereign risk can move towards risky or very high risky zone based on interactions with inflation rate and copula-based contagion measures. To our knowledge, we are the first to provide a variable selection among potential predictors for sovereign risk, also assigning specific risk thresholds for the selected key indicators at which the vulnerability of sovereigns becomes systemically relevant.

The rest of the paper proceeds as follows. Section 2 describes our data. Section 3 provides detailed information on our statistical procedures, the results and our inference methodology. We present our results in Section 4 and conclude with a brief discussion in Section 5.

2. Literature Review

According to the IMF, G-10 Report on Financial Sector Consolidation (2001), the systemic risk is the: "... risk that an event will trigger a loss of confidence measure of systemic risk". Embracing this definition, many papers focused on the identification of large and highly interconnected financial institutions (e.g. Bilio et al. (2012)), and how the failure of an institution can have a disastrous impact on the entire financial

system and economic activity (see Adrian and Brunnermeier (2011), Allen and Gale (2007) and Acharya et al. (2012), among others). Some other papers examine factors driving the systemic risk both in sovereign and corporate CDS data. Acharya et al. (2011) concentrate on the financial sector bailouts and, using a broad panel of bank and sovereign CDS data, show that bank and sovereign credit risk are intimately linked and conclude the latest banking and sovereign bailouts in Europe suggest that sovereign default risk has become closer and closer to that of their domestic banks.

Another strand of the literature explored comovements in financial markets. Among others, Christoffersen et al. (2012) apply a time varying copula model to capture nonlinear dependence among a large number of stock market indices, Lucas et al. (2014) conceive spillovers across countries through an increase in conditional default probabilities, Oh and Patton (2015) investigate systemic risk among a collection of corporate CDS spreads and Meine et al. (2016) measure the tail beta of a bank's CDS spread.

Strictly focused on the European sovereign debt crisis, much of the literature explored co-movements and major drivers in: (a) bond spreads (De Santis (2014), Beetsma et al. (2013), Favero (2013)); (b) sovereign credit default swaps (Longstaff et al. (2011), Kalbaskaa and Gatkowski (2012), Aizenman et al. (2013)); (c) spillover effects and feedback loop between European debt crisis and the financial sector (Acharya et al. (2010), Alter and Schuler (2012), DeBruyckerea et al. (2013); (d) sovereign risk contagion among Eurozone countries (Arezki et al. (2011), Beirne and Fratzscher (2013), Broto and Perez-Quiros (2015), Caporin et al. (2014), Mink and de Haan (2013) [2]).

[2]Early work on contagion is found by Allen and Gale (2000) who consider contagion arising from interbank cross holdings of deposits and Forbes and Rigobon (2002) who introduce a new definition of contagion between international assets after a crisis event.

Only recently, few studies examined the sovereign systemic risk in the Eurozone. Reboredo and Ugolini (2015) study systemic risk in European sovereign debt markets before and after the onset of the Greek debt crisis, using the conditional value-at-risk measure. Their results provide evidence that while the systemic impact of the Greek debt crisis is not so severe for non-crisis countries, systemic risk instead increases for countries in crisis. Ang and Longstaff (2013) explore systemic sovereign credit risk in the US and Europe using a multifactor affine framework. Their findings indicate strong heterogeneity among US and European issuers in their sensitivity to systemic risk and considerable evidence on the key role assumed by financial market variables. Manzo and Picca (2015) point out that while sovereign systemic risk has a large and persistent impact on the banking systemic risk, systemic banking risk has a smaller, transitory impact on systemic sovereign risk.

Finally, another strand of the literature which is more related to our study is concerned with changes in regimes occurring in the CDS dynamics. Caceres et al. (2010) analyse the reasons underlying the rising spreads during European crisis and argue that while during the early period of the crisis the main cause was risk aversion, in the later stages country-specific factors such as public debt and budget deficit played a primary role in the sharp rise in sovereign spreads. Arghyrou and Kontonikas (2012) find evidence confirming changes in regime for sovereign debt pricing with a dominant role assumed by country-specific macro-fundamentals during the crisis. Ait-Sahalia et al. (2014) propose a model to capture the dependencies among the risk of the different Eurozone countries and conclude that Eurozone CDS spreads, and hence default intensities, exhibit clusters in time and in space.

3. Data

The CDS is a typical example of an unfunded credit derivative that isolates and transfers credit risk only, hence its value reflects only the credit quality of the reference entity. The sovereign CDS are insurance-like contracts used to protect investors against losses on sovereign debt and are typically more liquid than the corresponding sovereign bonds (Longstaff et al. (2011)). We measure pairwise sovereign risk using 1505 daily quotes, over the period from 1 January 2008 to 7 October 2013, of the 5-yr sovereign CDS spreads for GIIPS, France, Germany and US. For the Greek CDS spread only 1414 quotes are available (Table 1). Since the end of 2009 and the start of 2010, the Greek CDS spread traded at extraordinary levels, even compared to its "alter-ego", the Portuguese CDS spread. On April 22, 2010, the Greek CDS spread reached the 700bps and afterwards the Greek CDS contracts have been converted to up front, as the protection seller had to pay up front a premium to the protection buyer, as the elevated Greek CDS basis mapped the sentiment of the market participants that the situation would be unsustainable in the long term. In the mean time, the volume of dealers quoting Greek CDS was not sufficient for the key providers of derivative pricing information to determine an official live price.

The proxies for estimating interconnections between each Euro sovereign CDS and financial intermediaries are the *US Banks 5-yr CDS index*, the *Euro Other Financials 5-yr CDS index* and *US Other Financials 5-yr CDS index*. Following Augustin et al. (2014), we consider macroeconomic factors in order to investigate their influence on sovereign CDS spreads. These are the *Debt/GDP ratio*, *exports/GDP ratio*, *GDP growth rate*, *industrial production*, *inflation* and the *unemployment rate*, chosen for each of the

countries in our dataset. Since their frequency is different from that of the CDS data, we repeat the same value until their new release. The sovereign CDS data are collected from Markit, the CDS indices from Thomson Reuters Datastream and the macroeconomic data from Eurostat. A full description of the identification of the indices and macroeconomic variables can be found in the Online Supplementary Material [3]

Table 1 summarizes the descriptive statistics of the daily CDS spreads. We verify the stylized facts addressed by Meine et al. (2016) and Augustin (2014). There is a substantial variability of the CDS spreads taking into account the values of the mean, minimum and maximum and the significant level of volatility. Fig.1 depicts the daily mean, minimum and maximum of the CDS spreads excluding Greece as the extreme high values of the Greek CDS spread would shade the properties of the rest of the series. The CDS spreads remained low at the outset of the crisis showing an upward trend from September 2008. Furthermore, the CDS spreads exhibit positive skewness (Fig.2) reflecting change in the risk appetite of the market participants. The high values of the first-order autocorrelation ACF(1) suggest strong autocorrelation and persistence.

4. Models

4.1. A flexible copula model for dependency

Arakelian and Dellaportas (2012) propose a flexible threshold model estimating bivariate copulas that change over time. Their work is based on the assumption that in different time periods, separated by thresholds, different volatilities and copula formulations can adequately explain the dependency between two financial assets. By assuming

[3] `https://dl.dropboxusercontent.com/u/109367329/ADSV_OnlineSupplementaryMaterial.pdf`.

Table 1: Daily sovereign CDS spreads and CDS indices from 1/1/2008 - 10/7/2013.

	Observations	Mean	StDev	Kurtosis	Skewness	Min	Max	ACF(1)
France	1505	80.65	57.09	3.05	0.91	6.15	247.31	0.9972
Germany	1505	43.67	26.08	2.89	0.72	5.01	115.67	0.9961
Greece	1419	2651.21	4124.95	7.10	2.08	20.66	25422.81	0.9879
Ireland	1505	327.06	258.31	2.47	0.77	14.69	1263.41	0.9979
Italy	1505	212.53	142.43	2.73	0.78	20.55	590.62	0.9967
Portugal	1505	427.50	393.30	2.78	0.94	17.41	1656.67	0.9983
Spain	1505	221.83	144.83	2.55	0.52	19.70	633.49	0.9967
US	1505	34.76	16.27	3.93	0.49	5.70	100.25	0.9888
Euro Banks 5-yr CDS index	1505	261.37	110.37	2.66	0.53	53.57	552.18	0.9961
Euro Other Financials 5-yr CDS index	1505	290.85	125.40	6.54	1.96	124.73	780.21	0.9956
US Banks 5-yr CDS index	1505	170.15	71.61	6.50	1.70	84.09	512.13	0.9870
US Other Financials 5-yr CDS index	1505	402.63	62.07	5.22	1.54	159.34	1099.70	0.9898

that the number and location of thresholds are unknown and need to be estimated, they create a model formulation consisting of all models with different volatilities, copula functions, number of thresholds and threshold locations. A reversible-jump MCMC algorithm is proposed which obtains samples from the posterior density of these models, and a Bayesian model-averaging estimation approach constructs a posterior density of Kendall's τ (Kendall (1938), Joe (1997), Nelsen (1999)), marginalised over all models and parameters within each model. Arakelian and Dellaportas (2012) propose the use of the posterior mean of this density as a measure of the dependency of two assets. Their empirical study explains interesting contagion effects in the Asian and Mexican crises.

We adopt the same model formulation and influential procedure here to provide a measurement of dependency between Euro sovereign CDS. There is only one difference from the implementation proposed by Arakelian and Dellaportas (2012), which it will be now described in detail. When we apply the reversible-jump MCMC algorithm to some CDS pairs, we notice that the mixing of the Markov chain over the product space of models and parameters was not satisfactory. We therefore adopt the population-

based simulation suggested by Jasra et al. (2007). This method generates L parallel-sampled auxiliary Markov chains with target densities $\pi_l \propto \pi^{\zeta_l}$, where π denotes the posterior density from which we need to obtain samples and ζ_l are ordered parameters $0 < \zeta_l < \zeta_{l-1} < \ldots < \zeta_1 < 1$. The densities π_l serve as independent Metropolis-Hasting proposal densities for the main chain with target density π. At each iteration, one auxiliary density π_l is chosen at random and used together with the current sampled point of l at the usual acceptance ratio of the main chain. In the terminology of Jasra et al. (2007), this is an exchange move in the population reversible-jump algorithm. We use the strategy proposed by Jasra et al. (2007), whereby five auxiliary chains are chosen with values of ζ_l being updated as a linear function of their past value and the acceptance rate of the process calculated within the burn-in period. We develop a MATLAB code to implement the method. The MCMC is computationally intensive as it takes 96 hours to converge when run on an Intel core i7, 8GB RAM computer. Convergence plots and specific details of the copulas used and the MCMC algorithm can be found in the Online Supplementary Material[4]

4.2. Regression Trees and Random Forest

Regression trees are nonparametric models constructed by recursively partitioning a data set with the values of its predictor variables with the objective of optimally predicting a response variable which can be continuous. Regression trees uncover forms of nonlinearity and identify multiple data regimes from a set of predictor variables. This approach is applied in the context of financial crisis studies (for example, see Manasse and Roubini (2009), Savona and Vezzoli (2015)) to study the complex and nonlinear

[4] `https://dl.dropboxusercontent.com/u/109367329/ADSV_OnlineSupplementaryMaterial.pdf`.

nature of financial crises as well as to create an early warning system with the aim of signalling impending crises when preselected leading economic indicators exceed specific thresholds.

Mathematically, having data consisting of R inputs and a continuous response, Y, for each of N observations, the algorithm needs to decide on the splitting variables, the split points, and the topology (shape) of the tree. To do this, the algorithm partitions the input space $\mathcal{S}$, namely the set of all possible values of $\mathbf{X}$ ($\mathbf{X} \in \mathcal{S}$), into disjoint regions T_k with $k = 1, 2, \cdots, K$, so that $\mathcal{S} \subseteq \bigcup_{k=1}^{K} T_k$. The underlying response-predictor structure $f(\mathbf{X})$ is represented by the piecewise constant functions g_k fitted over the input subspace:

$$f(\mathbf{X}) = \sum_{k=1}^{K} g_k I(\mathbf{X} \in T_k). \tag{1}$$

The sum of squares $\sum(Y - f(\mathbf{X}))^2$ is used as the criterion of minimization (Hastie et al. (2009)), thus obtaining a mapping of the response variable which is optimal for the number of final clusters, the best predictors and corresponding thresholds, and the predictions for the Y variable.

Regression trees are conceived with the aim of improving out-of-sample predictability. To achieve this, they are estimated through a cross-validation estimation procedure whereby the sample is partitioned into subsets, so that the analysis is initially performed on a single subset (the training sets), whereas the other subsets are retained for subsequent use in confirming and validating the initial analysis (the validation or testing sets). We adopt an ensemble learning inference procedure to strengthen our inferences: the random forest. This algorithm is a collection of regression trees using different combinations of variables and samples, so that predictions are more stable and less prone to

estimation errors. Details of the implementation of the random forest algorithm can be found in Breiman (2001). In summary, the idea is that the random forest algorithm combines regression trees built using bootstrap samples. Instead of splitting each node by using the best split among all variables, the random forest splits each node by picking out the best from a subset of predictors randomly chosen at that node, see Breiman (2001), Breiman (2003). The R software's package "tree" is used to implement the regression trees.

5. Results

5.1. Copula-based dependencies

We apply our threshold copula model to compute pairwise correlations in the form of Kendall's τ dependencies to daily differences in Euro sovereign CDS and CDS indices. The Markov chain is initiated with a model with zero breaks and, after a burn-in period of 10^6 iterations, a Markov chain output is obtained by collecting the next of 2.5×10^5 samples. Fig.3 reports the model-averaged posterior mean of Kendall's τ for all pairwise dependencies of the seven Euro sovereign CDS. Some of the preliminary findings are particularly interesting. In all the sub-figures of Fig.3, it is clear that a first jump in Kendall's τ occurred in mid-2008 little after the collapse of Bear Stearns, followed by a structural change in the dependence structures around the end of the same year with the collapse of Lehman Brothers. The period from 2009 to the first quarter of 2011 was characterised by strong contagion, with Kendall's τ around 0.6 in median, with low dispersion across all pairwise dependencies. After that, the overall Euro sovereign contagion seemed to decrease, as shown by the cross-dispersion, which increased until the end of the period, when the median Kendall's τ is around 0.4, close to the same values

exhibited early in 2008 but with higher cross dispersion. Fig.4 summarises such dynamics, depicting the cross-median, the minimum, the maximum and the cross-standard deviation. Fig.5 shows trends in US sovereign dependencies that are similar to those in Fig.3, however with very low values starting from the end of 2011. Interconnections with CDS indices show cyclical tendencies with significant spikes in dependencies with the banking sector both in Europe and the US (Fig.6) occurring in 2008, 2009 and 2010, and a rebound in 2012. For the *Euro Other Financials 5-yr CDS index* (Fig.6), the patterns are quite similar to sovereign-banking dependencies, while the *US Other Financials 5-yr CDS index* shows a downward trend from the peak in 2008 to the end of the period, with the exception of Greece, which presents very high values from 2011 onwards.

5.2. Sovereign risk and CDS dependencies

We first inspect how the level of each sovereign CDS is affected by each pair of Kendall's τ dynamics, in order to understand which of the pairwise dependencies exert the higher impact on sovereign risk dynamics. To avoid reverse causality among all pairwise Kendall's τ to be used as covariates, we exclude those dependencies that involve countries whose sovereign CDS dynamics are investigated. We run the random forest algorithm computationally and obtain the relative importance measures attributed to all single Kendall's τ by all countries. These measures are provided by the random forest algorithm as a natural way of ranking the importance of the variables in a regression tree setup; for details, see Breiman (2001), Breiman (2003). Fig.7 depicts the box plots of the variable importance measure (VIM), expressed on a scale 1-100, of each pairwise dependence. The dependencies between Italy and France, Spain and Portugal and Spain and Italy seem important in all CDS spreads, implying that they are key elements of

systemic risk in the Eurozone.

When considering the sovereign CDS spreads dynamics as a whole, the results are in line with the recent findings of Gonzlez-Hermosillo and Johnson (2014), in that Spain and Italy show considerable co-dependence in explaining each other's volatility, while Greece assumes a scant role as primary contagion channel. Our results indeed indicate that on average, the contribution of Greece only appears when considering co-evolution with Germany, although its importance is modest when compared with other dependencies (see Fig.7). As discussed by Gonzlez-Hermosillo and Johnson (2014), the mechanisms underlying the contagion propagation can follow very complex channels that are not related only to pure sovereign risk interconnections. Contagion can arise because of adverse market price dynamics, adverse cycles of worsening liquidity problems and connections with the financial sector (banks and other financial intermediaries). The challenging issue separating all these central factors and then understanding all possible risk patterns and corresponding triggers. This is exactly the theme of the next section, which is devoted to detecting systemic sovereign risk zones, shedding light on their deep-rooted causes, dynamics and risk signals.

5.3. Risk mapping

It is of particular interest to look over all the data simultaneously in a panel-data regression tree approach. Our response variable is all the European sovereign CDS spreads stacked together on a 10444×1 dimensions response, variable Y, and all Kendall's τ estimates are used as covariates, taking care again to avoid reverse causality. The dimension of the predictor matrix is 10444×21. We therefore stratify the systemic sovereign risk using country-specific fundamentals and contagion-based measures and attributed the

time-varying importance to all variables, thereby ranking all indicators over time. The final regression tree, which we assemble using the entire panel data, allows a clear understanding of the different risk regimes which are endogenously detected by the same algorithm. Note that no a-priori knowledge about the timing of the shifts is assumed. The concept of regime and connected changes is used here as a spatio-temporal risk stratification, leading to a number of final risk zones that include important insights in terms of their time-varying composition and the values assumed by the leading variables selected by the algorithm. To give an overview of the distributions taken on by all variables within each final node and not only of those selected by the regression tree, we hierarchically cluster the standardised values assigned to each variable within each final node and arrange them in ascending form, based on their ranking obtained through their arithmetic mean; see Fig.8.

Next, the analysis involves regression trees and random forest by using the level of the daily CDS for all seven Euro countries as dependent variables and the contagion-based measures and country-specific fundamentals selected based on the more relevant academic studies on this subject as covariates; see Section 1. Specifically, the set of possible leading indicators contains fourteen variables distinguishing between contagion-based and fundamental-based measures, as follows. The contagion-based measures, namely nonparametric daily pairwise dependencies are computed through Kendall's τ for each of the seven sovereign CDS: the Kendall's τ between France and Germany ($\tau_{Fr,Ger}$) representing the strength and the direction of association that exists between core countries; the Kendall's τ between all the pairs of GIIPS (τ_{GIIPS}), capturing the strength and direction of association between the peripheral countries; the Kendall's τ between a single and the rest of the group of European countries ($\tau_{EuroSvgn,EuroSvgn}$) represent-

ing a synthesis of the European dependencies from the perspective of a single country; the Kendall's τ between a single sovereign CDS and the *Euro Banks 5-yr CDS index* ($\tau_{svgn,EUBanks}$) assessing the sovereign and European banking system loop dynamics; the Kendall's τ between a single sovereign CDS and the *Euro Other Financials 5-yr CDS index* ($\tau_{svgn,EUOther}$), the Kendall's τ between a single sovereign CDS and the sovereign US 5-yr CDS ($\tau_{svgn,US}$) assessing the connections with the US sovereign risk dynamics; the Kendall's τ between a single sovereign CDS and the *US Banks 5-yr CDS index* ($\tau_{svgn,USBanks}$) assessing the sovereign-US banking system loop dynamics; the Kendall's τ between a single sovereign CDS and the *US Other Financials 5-yr CDS index* ($\tau_{svgn,USOther}$). The country-specific fundamentals are the *Debt/GDP ratio*, *exports/GDP ratio*, *GDP growth*, *industrial production*, *inflation* and the *unemployment rate*.

5.3.1. Inside the risk zones

Fig.8 shows the resulting regression tree computed using the overall panel data as a whole. The final model is based on eight variables out of fourteen potential leading indicators (eight contagion-based variables and six country-specific fundamentals): the Kendall's τ between the single sovereign CDS and GIIPS's CDS ($\tau_{svgn,GIIPS}$); the Kendall's τ between the single sovereign CDS and the rest of the Euro sovereign CDS ($\tau_{svgn,EuroSvgn}$); the Kendall's τ between the single sovereign CDS and the *Euro Other Financials 5-yr CDS index*($\tau_{svgn,EUOthFin}$); the Kendall's τ between the single sovereign CDS and the sovereign *US 5-yr CDS* ($\tau_{svgn,US}$); the *Debt/GDP ratio*, *GDP growth*, *inflation* and, the *unemployment rate*.

Hence, the overall sovereign systemic risk in the Eurozone can be stratified using four

contagion-based variables and four country-specific fundamentals. There are seventeen final nodes, although the corresponding mean values of the expected CDS spreads allow us to make some grouping based on specific risk levels, from low to very high, as explained below. We inspect each of the seventeen risk regimes from a number of perspectives, such as in terms of the expected CDS spread, the threshold values computed by the algorithms and the time-varying country composition of each node, looking primarily at the values assumed both by leading covariates and those that are potentially informative, to come up with a complete "genetic" mapping of each risk zone. With the objective of inspecting the anatomy of each final node, we follow a visual mining philosophy thereby reducing data interpretation complexity through visualization. Specifically, we refer to heatmaps, commonly used to emphasize data that are above or below a threshold as "hot" or "cold" colors, respectively. The heatmaps are widely used in biology for gene representation which is similar to our aim in representing the inner (say, genetic) mapping of final nodes in terms of how the selected predictors of sovereign risk are expressed, moving from low values (cold colors) to high values (hot colors). Predictor values are standardized to avoid different scale orders, and depicted by a rectangular tiling of different colors within the data matrix. In our analysis, low values (cold colors) are in blue, high values (hot colors) are in red, while values around the mean (warm colors) are in yellow. Heatmaps also compute two hierarchical cluster analyses: one is being implemented on the contagion-based variables and country-specific fundamentals and the other one on the observations (more precisely, on the countries in correspondence to different years), thereby realizing two dendrograms appended on the x- and y-axes, respectively (Ling (1973)). In doing this, the columns and the rows of the data matrix are permuted based on column and row means. In this way, similar values are placed near each other according to the clustering

algorithm used in the analysis (Sneath (1957)).

Based on this thorough analysis, we develop a comprehensive sovereign systemic risk regimes mapping. There is a simple way of reading the risk paths shown in the regression tree: by starting from the top node (in our case τ_{GIIPS}) and using the corresponding splitting rule ($\leq$ or $>$), we check if the value of the variable within the node agrees with the splitting rule: if "yes", the move is to the left, otherwise, it is to the right. Once the next node is reached, based on a new variable and a new splitting rule, the move is to the left or to the right. This process leads to the final nodes, where the expected value of the dependent variable are given.

A notable result we obtain is the discrimination performed by the regression tree between two main macro-regions through the τ_{GIIPS} indicator (the Kendall's τ with GIIPS's CDS),which is placed at the top of the tree with a threshold value of 0.3167. The two macro-regions detected based upon the value assumed by such indicator are: (a) a macro area, called *Greek Only Area*, corresponding to values of the τ_{GIIPS} which is placed at the top of the tree with a threshold value of 0.3167, leading on the right of the tree towards extremely high risk levels, where the values of expected CDS in each final node range from 1515 bps to 24706 bps; and (b) a macro area, called *Euro Systemic Sovereign Risk Area* corresponding to values of the τ_{GIIPS} indicator greater than 0.3167, leading to different risk zones spanning from low (76 bps) to high risk levels (1217 bps).

5.3.2. The Greek Only Area

(a) High sovereign dependency with moderate financial contagion: Unlike the previous risk zone, here high Kendall's τ with all Euro sovereign CDS ($\tau_{EuroSvgn,EuroSvgn}$) greater than 0.5209 moves together with Kendall's of sovereign CDS with the *Euro*

Other Financials 5-yr CDS index ($\tau_{svgn,EUOthFin}$) less than 0.4606, and inflation rate less than 1.9%: following this risk path, the expected CDS spread is dramatically high and equal to 24706 bps. The expected sovereign risk tends to be less pervasive when inflation is greater than the selected threshold, and it currently reaches the level of 7726 bps. Looking at the corresponding heatmaps reported in Fig.9, we note that for both final nodes the Kendall's τ with *US Banks 5-yr CDS index* is high for both final nodes, in addition to high values for the unemployment rate and Debt/GDP ratio.

(b) High sovereign dependency with high financial contagion: Unlike the previous risk zone, here high Kendall's τ with the Euro sovereign CDS ($\tau_{EuroSvgn,EuroSvgn}$) moves in tandem with high Kendall's τ of sovereign CDS with the *Euro Other Financials 5-yr CDS index* ($\tau_{svgn,EUOthFin}$) and GDP growth with inflation lead to different sovereign risk values: when GDP growth is higher than 6.85%, the expected CDS is 14888 bps; instead when the GDP growth is below 6.85%, an upward moving inflation (more than 2.95%) leads to 2156 bps against 9328 bps, which is the expected CDS value when inflation is low (and less than 2.95%). Heatmaps for the three final nodes (see Fig.9) confirm the high financial contagion by showing high values for dependencies with *US* and *Euro Other Financials 5-yr CDS index* as well as *US Banks 5-yr CDS index*.

(c) Contained sovereign dependency: in this risk zone is the Kendall's τ of the Euro sovereign CDS spread less than 0.5209. The final nodes ultimately depend on inflation, for which deflation states seem to contain CDS turbulence, as the expected CDS spread is 1515 bps when inflation is less than -0.25%, whereas having inflation

that is greater than the selected threshold leads to a slightly higher level of sovereign risk. The corresponding heatmap highlights high values for unemployment rate and Debt/GDP ratio.

5.3.3. The Euro systemic sovereign risk area

This macro area includes many risk regimes that together well stratify the Euro systemic sovereign risk area for all the seven countries over the entire period, but clearly with the exception of Greece during the period from June 2011 to October 2013. As discussed above, this macro area is identified by values of the median Kendall's τ with GIIPS greater than 0.3167. Next, based on other leading indicators selected by the regression tree, the splits that follow lead to 10 final nodes that can be grouped into three main risk zones.

(a) Safe Zone: This regime exhibits low unemployment rate (less than 11.75%) and moderate public indebtedness relative to GDP (Debt/GDP ratio$<$ 119.6%), and expected CDS spread is 76 bps. This is the lower value among all the final nodes and some very interesting insights can be gained by inspecting the time-varying country composition, which completely changed as the crisis began to unfold. Fig.10 reports the country composition and the heatmap. The country composition is identified by observing the CDS values with corresponding country names for each node on a monthly basis.

For this safe zone regime, we observe that all seven countries are included in this cluster from January 2008, and only starting from September 2008, when the Lehman Brothers collapsed, did non-safe countries begin to leave this regime. The first country moved to other regimes was Spain in September 2008, followed

by Greece in April 2009, Ireland in May 2009, Portugal in May 2010, and Italy in September 2010. Starting from 2011, only France and Germany remained in the safe zone until the end of the period. These findings confirm the "wake-up call" phenomenon in the Eurozone (Goldstein (1998), Goldstein et al. (2000)), since markets ignored deteriorating fundamentals during times of non-crisis and became highly sensitive upon onset of crisis. The novelty of our results is twofold. Firstly, markets became highly sensitive to Debt/GDP ratio together with unemployment rate, and secondly, related to the first point, the values signalling an impending change in regime out of the safe zone are known for such indicators, namely an unemployment rate greater than 11.75% or a Debt/GDP ratio greater than 119.6%. In both scenarios, a move towards risky or high-risk zones is expected.

(b) Risky Zone: this risk regime is characterised by a low unemployment rate with high Debt/GDP ratio or with a high unemployment rate and includes the following subzones: the low unemployment rate with high Debt/GDP ratio scenario and the high unemployment rate scenario. In the first scenario, inflation enters the risk stratification process by splitting between low (less than 3.15%) and moderate (greater than 3.15%) inflation, leading to an expected CDS spread of 219 bps and 445 bps respectively. The time-varying country compositions (Fig.12) of the two final nodes and the heatmaps (Fig.13) highlight some further interesting differences in more depth.

The first node, showing an expected CDS value of 219 bps, includes Greece from March 2009 to March 2010, and Italy from September 2010 to September 2011 (excluding January and February 2011) and October 2012 to January 2013. The

corresponding heatmap shows low values for exports/GDP ratio with high values for contagion-based measures, specifically the Kendall's τ with France and Germany and with GIIPS. The second node, showing an expected CDS value of 445 bps, again includes Greece, from April to May 2010, and Italy, from September 2011 to October 2012. Looking at the corresponding heatmaps, we note high values for the Kendall's τ with France and Germany on the one hand, and on the other, low values for Kendall's τ with of the Euro sovereign CDS with *US Other Financials 5-yr CDS index* ($\tau_{EuroSvgn,USOthFin}$). In other words, it seems that the form of contagion that really matters concerns dependency with the core countries of the Eurozone - France and Germany - together with high Debt/GDP ratio and moderate inflation. If we consider these findings together, it is of particular interest that the first effects on the re-pricing of sovereign risk in Greece, occurring at the end of 2009 and continuing with the spike of the CDS from April to May 2010 when Greece applied for financial support, were the same in terms of their underlying contagion-based and fundamental-based triggers as those for Italy from September 2010 to January 2013. The second scenario includes three final nodes which modulate between low (less than 66.45%) and moderate (between 66.45% and 93.65%) Debt/GDP ratio, and also point to high Debt/GDP ratio with low dependency with other Eurozone sovereign risks dynamics. In the first sub-scenario, the corresponding heatmaps display for both nodes (with expected CDS spread 160 bps and 370 bps, respectively) high values for Euro sovereign contagion (Kendall's τ with GIIPS and France and Germany) and Euro banking contagion (Kendall's τ of sovereign CDS with the *Euro Banks 5-yr CDS index*, $\tau_{svgn,EUBanks}$). By observing the country composition over time, we note that Spain and Ireland were in both nodes,

while Portugal was in the final node only, with moderate Debt/GDP ratio. In the second sub-scenario, corresponding to the final node with 285 bps as expected sovereign risk level, the heatmap displays low values for US financial contagion and industrial production, thereby mixing contagion-based and fundamental-based indicators. This was the case for Portugal and Italy over the November 2012-October 2013 period (see Fig.12) which saw high values for Debt/GDP ratio and unemployment rate moving with low contagion. This explains why the sovereign risk was slightly lower than it was for Ireland, Spain, and Portugal, clustered within the node with 370 bps as expected CDS spread: in such a case, moderate public indebtedness was associated with significant sovereign and banking contagion.

(c) High Risk Zone: the main features of this very dangerous zone (see Fig.14), which leads towards very high sovereign risk levels, are high unemployment rate (greater than 11.75%), together with high Debt/GDP ratio (greater than 93.65%) and significant sovereign contagion (Kendall's τ of Euro sovereign CDS greater than 0.4872). Taken together, these indicators with corresponding red flags signal extreme risk sensitivity, which is reflected into expected CDS spreads spanning from 575 bps to 1217 bps covering four final nodes. We identified the following two sub-zones based on such a final risk partition:

(1) *The GIIPS contagion scenario*: In this scenario the median Kendall's τ between GIIPS is greater than 0.4924 and leads towards two final nodes. The first denotes high dependency with *Euro Other Financials 5-yr CDS index* and low GDP growth; see Fig.15. Discontinuously, Greece (May-June 2010), Portugal

(January-May 2011[5] and September-October 2012), Spain (November 2011-October 2012) populated this node which exhibit 575 bps as expected risk level. The second node which denotes higher risk, and specifically 842 bps, is similar to the previous one but differs because of its low dependency with *Euro Other Financials 5-yr CDS index* (see Fig.15). This was the case for Greece (from July 2010 to March 2011), Ireland (from April 2011[6] to October 2011), and Portugal (from May to June 2011), as depicted in Fig.14 showing the country composition over time. (2) *The low US-based sovereign dependency*: Here, the two final nodes show significant risk level shift, since the first exhibits 717 bps and the second 1217 bps. While both nodes are characterised by extremely low (first node) or low (second node) Kendall's τ towards the sovereign US 5-yr CDS spread dynamics, looking at the corresponding heatmaps (Fig.15), we observe that what probably reflects higher risk is the Kendall's τ of sovereign CDS with the *US Other Financial 5-yr CDS index* ($\tau_{svgn,USOthFin}$). Indeed, the second node includes high values for Kendall's τ of sovereign CDS with the with *US Other Financials 5-yr CDS index*, in particular for some parts of the final partition (as it is discussed below corresponding to Greece), while the first node shows low values for this indicator. In fact, this different dependency towards *US Other Financials 5-yr CDS index* dynamics arises when observing the country composition of the two final nodes with corresponding time series of such a variable. Portugal and Ireland are placed within the node with expected CDS spread at 717 bps, from June to October 2012. During this period both countries exhibited extremely low values of Kendall's τ of sovereign CDS with

[5]Portugal applied for financial support in April 2011.

[6]Ireland is already in financial support program since November 2010.

the *US Other Financials 5-yr CDS index* ($\tau_{svgn,USOthFin}$) around 0.03. On the other hand, Greece and Portugal are within the node with 1217 bps as expected CDS spread for the period from March 2011 to June 2012 (Greece: March-June 2011; Portugal: July 2011-June 2012). During this period, the values of Kendall's τ of sovereign CDS with the *US Other Financials 5-yr CDS index* ($\tau_{svgn,USOthFin}$) were on average around 0.16 with a big difference between Greece, that shown an average value of 0.46, and Portugal that shown an average of 0.09.

5.3.4. Risk Indicators and their Importance

The risk stratification performed by means of the regression trees analysis give us the indicators with their thresholds computed over the entire period of January 2008-October 2013, throughout which the different risk zones are identified. To get a more clear understanding of the importance assumed by all the fourteen indicators, we run the random forest algorithm on a monthly basis and compute the VIM for each variable, thereby obtaining a distribution of the corresponding scores, as we report in Fig.16 and 17. In this way, we better explore the role assumed by all variables in terms of their impact on systemic sovereign risk dynamics and examine how contagion-based and country-specific indicators exerted different impacts over time.

Debt/GDP, inflation and GDP growth rate have the highest median among the country-specific fundamentals, although inflation demonstrates great variability in terms of upper-lower quartile range as we also observe with their time series, which presents a substantial drop during the sub-period from June 2011 to March 2012. Unemployment rate seems to be the less influential indicator both in terms of median, and upper-lower quartiles, which are lower than other fundamentals looking at the box plot and

the relative median value. However, the corresponding time series further highlights the behaviour of the importance of the variable over time, since in November 2009, November-December 2010, and from September 2012 until the end of the period, the indicator appears to be an extremely important variable, presenting near maximum values. This finding also details the results of the final regression tree, in which the variable assumed great importance in detecting some of the main systemic sovereign risk zones. Indeed, the VIM analysis provides evidence of the fact that the unemployment rate is only relevant in specific time periods. With this analysis, we are able to explain the complex and nonlinear nature of the systemic sovereign risk, together with Debt/GDP, inflation and sovereign contagion dependencies. The ranking of the contagion-based indicators highlights the great importance assumed by *US Other Financials 5-yr CDS index* ($\tau_{svgn,USOther}$) and *Euro Other Financials 5-yr CDS index* ($\tau_{svgn,EUOther}$), while *Euro Banks 5-yr CDS index* ($\tau_{svgn,EUBanks}$) and *US Banks 5-yr CDS index* ($\tau_{svgn,EUBanks}$) dependency appear to have a low impact on systemic sovereign risk dynamics. However, the box plot for *Euro Banks 5-yr CDS index* dependency highlights some outliers positioned at the top of the scale, thus demonstrating great impact in some specific periods. This was clearly the case from March to May 2008 (collapse of Bear Stearns) when the variable assumed the highest VIM value, and from December 2011 to May 2012 (the ECB suspended use of Greek bonds as collateral in February 2012, and Greece defaulted in March 2012), with values around and equal to the maximum (see Fig.17). Sovereign dependency shows increasing importance over time for GIIPS and core countries (France and Germany) as well as for the US, as we can see in the corresponding time series, which indicates very high VIM values starting from 2010, namely when the Euro debt crisis erupted with Greek CDS spikes, followed by those of other GIIPS countries. To

examine the importance assumed by the variables clustered according to contagion and macro fundamental types, we extract the first principal component (pc) from the VIM of the first subgroup (*pc-contagion*) of the eight contagion-based variables, $\tau_{Fr,Ger}$, τ_{GIIPS}, $\tau_{EuroSvgn,EuroSvgn}$, $\tau_{svgn,EUBanks}$, $\tau_{svgn,EUOther}$, $\tau_{svgn,US}$, $\tau_{svgn,USBanks}$, $\tau_{svgn,USOther}$, and from the VIM of the second subgroup (*pc-macro*) of the six country-specific macro fundamentals, Debt/GDP, exports/GDP ratio, GDP growth, industrial production, inflation, unemployment rate. The two principal components are reported in Fig.18 and show interesting patterns over time. Specifically, we observe that contagion-based variables, summarized by *pc-contagion*, assumed an increasing importance starting from the third quarter of 2008 (the Lehman Brothers collapse) until the first quarter of 2011.

In such a period, fundamental-based variables, summarized by *pc-macro*, assumed an opposite tendency, with a drop in importance during 2008 (around the collapse of Bears Stearns) with moderate importance throughout the end of 2009. Afterwards, and specifically starting from 2010, importance grew progressively with a peak at the end of 2011, before next showing a large drop in the second quarter of 2012, but quickly returned to high values, moving in tandem with contagion-based variables until the end of the year. After that, both importance metrics showed a downtrend towards their median at the end of the period. These results therefore confirm a time-varying importance assumed by fundamentals, which became relevant with the Greek crisis and contagion-based factors: (1) which assumed a key importance with the Lehman Brothers collapse, (2) that achieved new emphasis with the Euro debt crisis erupted in 2010, (3) that exhibited a temporary setback during 2011, but, (4) that became relevant again with the same impact of fundamental variables starting from 2012 and and (5) finally flexing towards a median reverting level at the end of the period together with fundamental-based

variables.

6. Conclusions

Since the start of the financial crisis of 2008 and thereafter in the European debt crisis, the sovereign credit default swaps (CDS) have played an important role as they have acted as measures of sovereign default risk by the participants of the financial markets. The variability of CDS spreads among countries and the tendency of some of them to move together, raised fears of contagion and questions as to the existence of systemic risk among them.

We propose a novel framework identifying sovereign systemic risk zones. In a first step, we explore the cross-dynamics of sovereign CDS in terms of time-changing contagion measures based on copulas. In a second step, these measures are assembled together with country-specific fundamentals, thereby identifying the leading indicators with corresponding red flags, which are valuable in stratifying sovereign systemic risk in different risk regimes. Using data on Greek, Irish, Italian, Portuguese, Spanish, French and German sovereign CDS over the period 2008-2013, our empirical analysis provided important findings on the origin and dynamics of sovereign systemic risk.

First of all, we find that Greece is a "world apart" from July 2011 to the end of the period, when the country started showing very low dependencies with other peripheral Euro countries with very high levels of CDS spreads mapped onto extremely high values for unemployment rate and Debt/GDP ratio. Secondly, we identify three main systemic risk zones based on contagion and country-specific fundamentals: (1) a safe zone, characterised by low unemployment rate (less than 11.75%) and moderate public indebtedness relative to GDP (Debt/GDP ratio $< 119.6\%$), (2) a risky zone with high unemployment

rate, or with low unemployment rate coupled with high Debt/GDP ratio and (3) a high risk zone, where high unemployment rate (greater than 11.75%) moves together with high Debt/GDP ratio (greater than 93.65%) and significant sovereign dependency. Thirdly, we provide evidence on time-varying importance of fundamentals, which captured attention during the Greek crisis. Instead, contagion-based factors became critical close to the collapse of Lehman Brothers, accomplishing another accentuation due to the Euro debt crisis which erupted in 2010, and finally demonstrating the same importance as the fundamental-based variables.

These results have important policy implications for early detection and the causal identification of sovereign systemic risk. Indeed, providing valuable early warning signals may be extremely valuable for taking the right measures of prevention and intervention for countries that may move towards dangerous risk paths.

Acknowledgment

We would like to thank Pierluigi Balduzzi, Andreas Pick and the participants of Consortium for Systemic Risk Meeting Analystics Semi-Annual Meeting (2014) held at the Massachusetts Institute of Technology in Cambridge, Massachusetts, the SYRTO Conference on Systemic Risk, organised by the Finance and Econometrics departments of the VU University Amsterdam and held in Amsterdam on June 4-5, 2015, the SYRTO Final International Conference, organized by the Universite Paris1 Pantheon, Sorbonne and held in Paris on February 2016 for their beneficiary comments. The last three authors acknowledge funding from the European Unions Seventh Framework Programme (FP7-SSH/2007-2013) for research,technological development and demonstration under grant agreement no. 320270-SYRTO.

References

Acharya, V. V., Pedersen, L. H., Philippon, T. and Richardson, M. P., May 2010. Measuring Systemic Risk. AFA 2011 Denver Meetings Paper. Available at SSRN: http://ssrn.com/abstract=1573171 or http://dx.doi.org/10.2139/ssrn.1573171.

Acharya, V., Drechsler, I. and Schnabl, P., 2014. A Pyrrhic Victory? Bank Bailouts and Sovereign Credit Risk, Journal of Finance 69, 2689-2739.

Acharya, V., Engle, R. and Richardson, M., 2012. Capital Shortfall: A New Approach to Ranking and Regulating Systemic Risks, American Economic Review 102, 59-64.

Adrian, T. and Brunnermeier, M. K., CoVaR, September 2011. FRB of New York Staff Report No. 348. Available at SSRN: http://ssrn.com/abstract=1269446 or http://dx.doi.org/10.2139/ssrn.1269446.

Aizenman, J., Hutchison, M. and Jinjarak, Y., 2013. What is the risk of European Sovereign Debt Defaults? Fiscal Space, CDS Spreads and Market Pricing of Risk. Journal of International Money & Finance 34, 37-59.

Allen, F. and Gale, D., 2000. Financial Contagion. Journal of Political Economy 108, 1-33.

Allen, F. and Gale, D., 2007. Understanding financial crises, Oxford University Press, USA.

Alter, A. and Schuler, Y. S., 2012. Credit Spread Interdependencies of European States and Banks During the Financial Crisis. Journal of Banking & Finance 36, 3444-3468.

Ang, A. and Longstaff, F. A., 2013. Systemic Sovereign Credit Risk: Lessons from the U.S. and Europe. Journal of Monetary Economics 60, 493-510.

Arakelian, V. and Dellaportas P., 2012. Contagion Determination via Copula and Volatility Threshold Models. Quantitative Finance 12, 295-310.

Arezki, R., Candelon, B. and Sy, A. N. R. Sovereign Rating News and Financial Markets Spillovers: Evidence from the European Debt Crisis, IMF Working Paper, 11/68(2011), March.

Arghyrou, M. G. and Kontonikas, A., 2012. The EMU Sovereign-debt Crisis: Fundamentals, expectations and contagion. Journal of International Financial Markets, Institutions and Money 22, 658-677.

Ait-Sahalia, Y., Laeven, R.J. A. and Pelizzon, L., 2014. Mutual Excitation in Eurozone sovereign CDS. Journal of Econometrics 183, 151-167.

Augustin, P., 2014. Sovereign credit default swap premia. Journal of Investment Management. forthcom-

ing.

Augustin, P., Subrahmanyam, M. G., Tang, D. Y. and Qian Wang, S., 2014. Credit Default Swaps: A Survey, Foundations and Trends in Finance, 9, 1/2, 1-196.

Augustin, P. and Tedongap, R., 2014. Real economic shocks and sovereign credit risk. Journal of Financial and Quantitative Analysis, *forthcoming*.

Beetsma, R., Giuliodori, M., de Jong, F. and Widijanto, D., 2013. Spread the News: The Impact of News on the European Sovereign Bond Market during the Crisis. Journal of International Money and Finance 34, 83-101.

Beirne, J. and Fratzscher, M., 2013. The Pricing of Sovereign Risk and Contagion During the European Sovereign Debt Crisis. Journal of International Money and Finance 34, 60-82.

Bilio, M., Getmanskyb, M., Lo, A. W., Pelizzon, L., 2012. Econometric measures of connectedness and systemic risk in the finance and insurance sectors. Journal of Financial Economics 104, 535-559.

Breiman, L., 2001. Random Forests. Machine Learning 45, 5-32.

Breiman, L., 2003. Random Forests Manual v4.0, Technical report, UC Berkeley.

Broto, C. and Perez-Quiros, G., 2015. Disentangling Contagion Among Sovereign CDS Spreads During the European Debt Crisis. Journal of Empirical Finance 32, 165-179.

De Bruyckerea, V., Gerhardt, M., Schepens, G. and Vander Vennet, R., 2013. Bank/sovereign Risk Spillovers in the European Debt Crisis. Journal of Banking & Finance 37, 4793-4809.

Caceres, C., Guzzo, V. and Segoviano, M., 2010. Sovereign Spreads: Global Risk Aversion, Contagion or Fundamentals?, IMF Working Paper 10/120 .

Caporin, M., Pelizzon, L., Ravazzolo, F. and Rigobon, R., January 2014. Measuring Sovereign Contagion in Europe. Available at SSRN: `http://ssrn.com/abstract=2023756` or `http://dx.doi.org/10.2139/ssrn.2023756`.

Christoffersen, P., Errunza, V., Jacobs, K. and Langlois, H., 2012. Is the Potential for International Diversification Disappearing? A Dynamic Copula Approach. Review of Financial Studies 25, 3711-3751

Favero, C. A., 2013. Modelling and Forecasting Government Bond Spreads in the Euro area: a GVAR model. Journal of Econometrics, **177**, 343-356.

Forbes, K. J. and Rigobon, R., 2002. No contagion, only interdependence: Measuring stock markets comovements, *Journal of Finance* 57, 2223-2261.

Goldstein, M., 1998. The Asian Financial crises: causes, cures, and systemic implications, Institute for International Economics, Washington.

Goldstein, M., Reinhart, C. and Kaminsky, G., 2000. Assessing Financial Vulnerability: An Early Warning System for Emerging Markets, Institute for International Economics.

Gonzlez-Hermosillo, B. and Johnson, C. A., 2014. Transmission of Financial Stress in Europe: The Pivotal Role of Italy and Spain, But Not Greece, IMF Working Paper No. 14/76.

IMF, 2001, Group of Ten, Report on Consolidation in the Financial Sector.

Jasra, A., Stephens, D. A. and Holmes, C. C., 2007. On Population-Based Simulation for Static Inference. Statistics and Computing 17, 263-279.

Joe, H., 1997) *Multivariate Models and Dependence Concepts*, Monographs on Statistics and Applied Probability, 73, Chapman & Hall, London.

Kalbaskaa, A. and Gatkowski, M., 2012. Eurozone Sovereign Contagion: Evidence from the CDS Market (2005-2010). Journal of Economic Behavior and Organization 8, 657-673.

O' Kane, Dominic, Modelling Single-name and Multi-name Credit Derivatives, 2008, Wiley.

Kendall, M., 1938. A New Measure of Rank Correlation. Biometrika 30, 81-89.

Ling, R., 1973. A computer generated aid for cluster analysis. Communications of the ACM 16, 355361.

Longstaff, F. A., Pan, J., Pedersen, L. H. and Singleton, K. J., 2011. How Sovereign Is Sovereign Credit Risk?. American Economic Journal: Macroeconomics 3, 75-103.

De Luca, G., Rivieccio, G., and Zuccolotto, P., 2010. Combining Random Forest and Copula Functions: A Heuristic Approach for Selecting Assets from a Financial Crisis Perspective. Intelligent Systems in Accounting, Finance and Management 17, 91-109.

Lucas, A., Schwaab, B. and Zhang, X., 2014. Conditional Euro Area Sovereign Default Risk. Journal of Business and Economic Statistics 32, 271 -284.

Manasse, P. and Roubini, N., 2009. "Rules of Thumb" for Sovereign Debt Crises. Journal of International Economics 78, 192-205.

Manzo, G. and Picca, A., January 2015. The Sovereign Nature of Systemic Risk . Available at SSRN: `http://ssrn.com/abstract=2524991`.

Meine, C., Supper, H. and Weiß, G.N. F., 2016. Is tail risk priced in credit default swap premia? *Review of Finance* 20, 287-336.

Mink, M. and de Haan, J., 2013. Contagion During the Greek Sovereign Debt Crisis. Journal of Inter-

national Money and Finance 34, 102-113.

Nelsen, R.B., 1999. *An Introduction to Copulas*, Lecture Notes in Statistics, 139, Springer, New York.

Oh, D. H. and Patton, A. J., 2015. Time-Varying Systemic Risk: Evidence from a Dynamic Copula Model of CDS Spreads, working paper, Duke University.

Reboredo, J. C. and Ugolini, A., 2015. Systemic Risk in European Sovereign Debt Markets: A CoVaR-copula Approach. Journal of International Money and Finance 51, 214-244.

De Santis, R. A., 2014. The Euro Area Sovereign Debt Crisis: Identifying Flight-to Liquidity and the Spillover Mechanisms. Journal of Empirical Finance 26, 150-170.

Sneath, P.H. A., 1957. The Application of Computers to Taxonomy. *Journal of General Microbiology* 17, 20126.

Savona, R. and Vezzoli, M., 2015. Fitting and Forecasting Sovereign Defaults using Multiple Risk Signals. Oxford Bulletin of Economics and Statistics 77, 66-92.

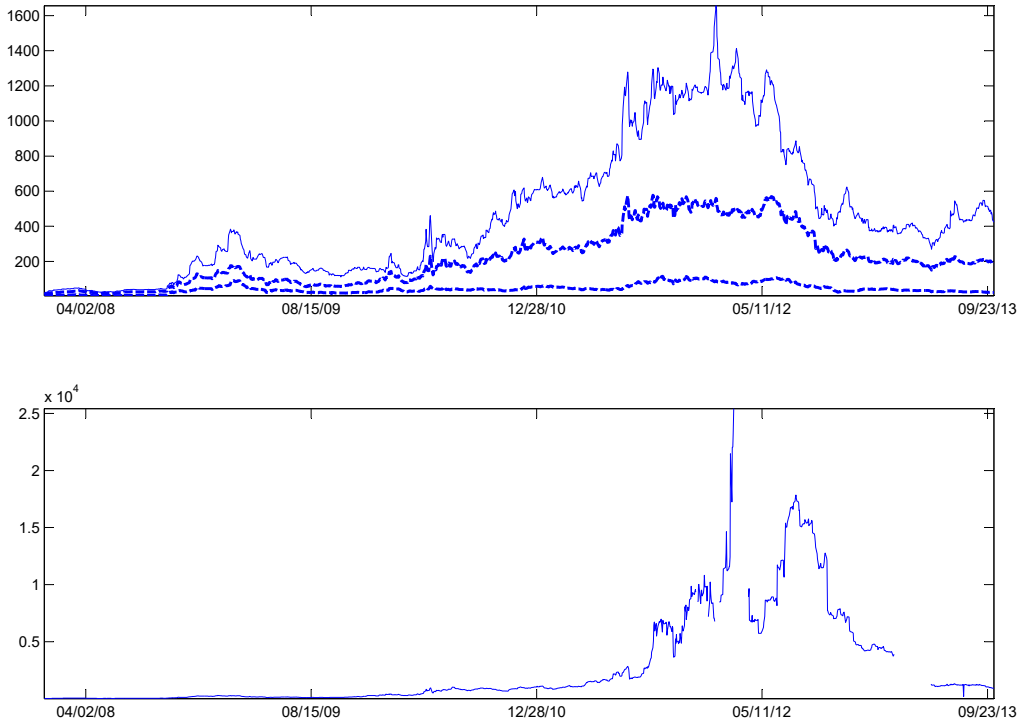

Fig. 1: *On the top*: Evolution of min(dashed-dotted line), mean(dashed line) and max(solid line) of France, Germany, Ireland, Italy, Portugal and Spain 5-yr sovereign CDS spread. *On the bottom*: Greek CDS spread.

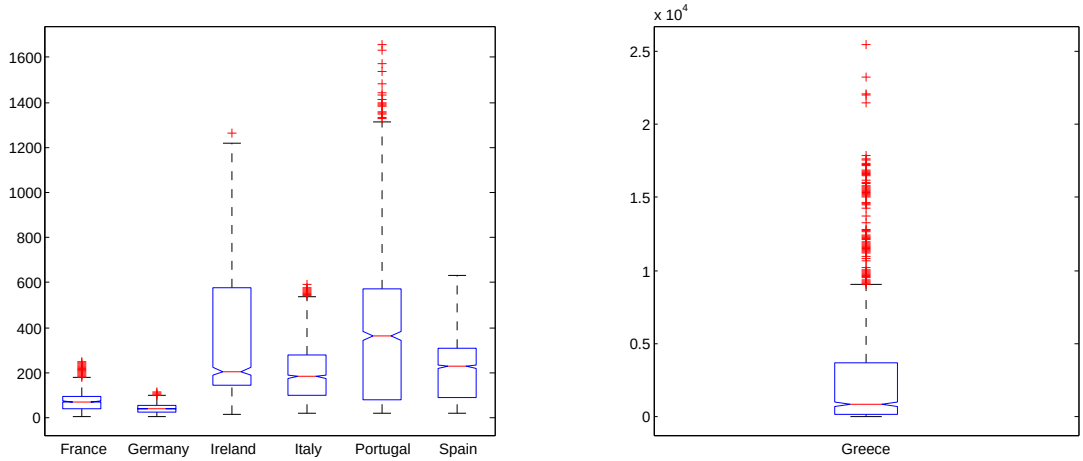

Fig. 2: Box plots of Euro sovereign CDS spreads from 1/1/2008 to 7/10/2013.

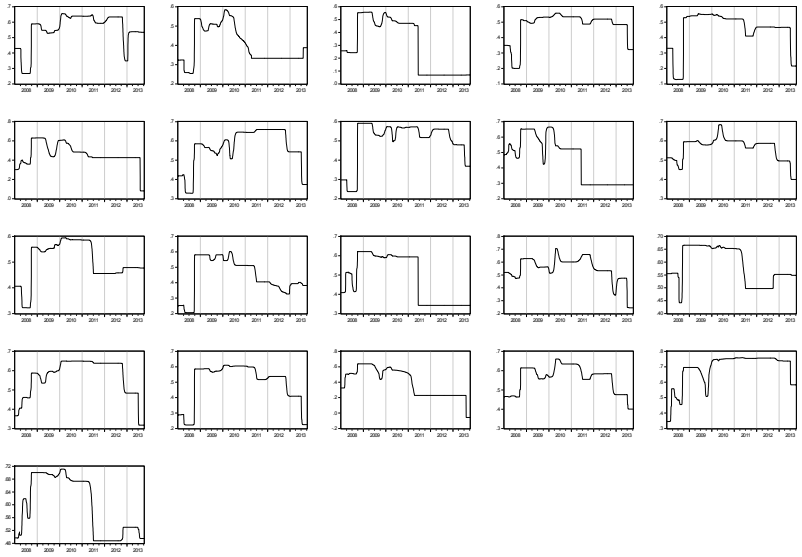

Fig. 3: Posterior averaged Kendall's τ. Beginning from the top left and moving to the right, Kendall's τ between sovereign CDS spreads of: Germany-France, Greece-France, Greece-Germany, Ireland-Greece, Italy-France, Italy-Germany, Italy-Greece, Portugal-France, Portugal-Germany, Portugal-Greece, Portugal-Ireland, Spain-France, Spain-Germany, Spain-Greece, Spain-Ireland, and Spain-Portugal.

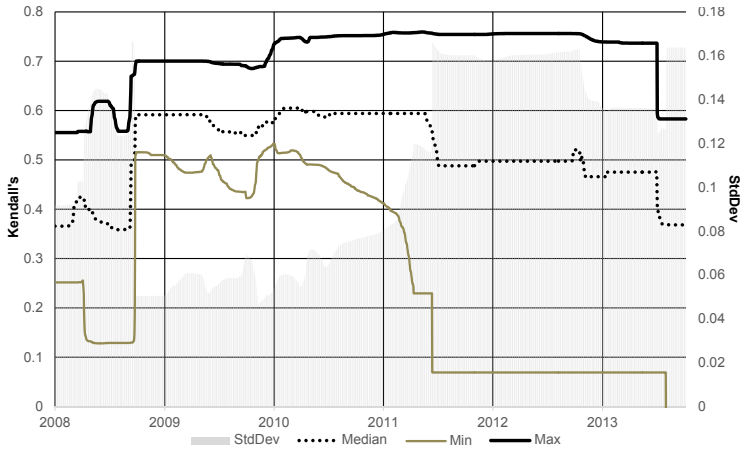

Fig. 4: Median (Median), minimum (Min), maximum (Max) and cross standard deviation (StdDev) of the pairwise Kendall's τ computed based on the Euro countries.

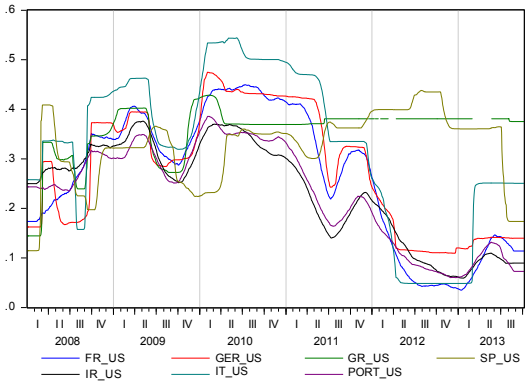

Fig. 5: Model averaged Kendall's τ computed for each Euro country (Greece (GR), Italy (IT), Ireland (IR), Portugal (PORT), Spain (SP), France (FR), Germany (GER)) relative to the sovereign US 5-yr CDS spread (US). Estimates for Greece have some missing values, as the corresponding sovereign CDS was not traded during those days.

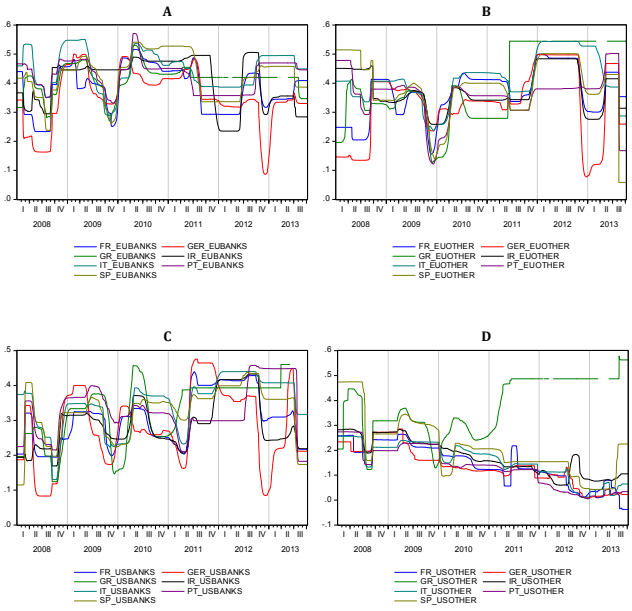

Fig. 6: Model averaged Kendall's τ computed for each Euro country (Greece (GR), Italy (IT), Ireland (IR), Portugal (PT), Spain (SP), France (FR), Germany (GER)) relative to: (A) the *Euro Banks 5-yr CDS index* (EUBANKS); (B) the *Euro Other Financials 5-yr CDS index* (EUOTHER); (C) the *US Banks 5-yr CDS index* (USBANKS); (D) the *US Other Financials 5-yr CDS index* (USOTHER).

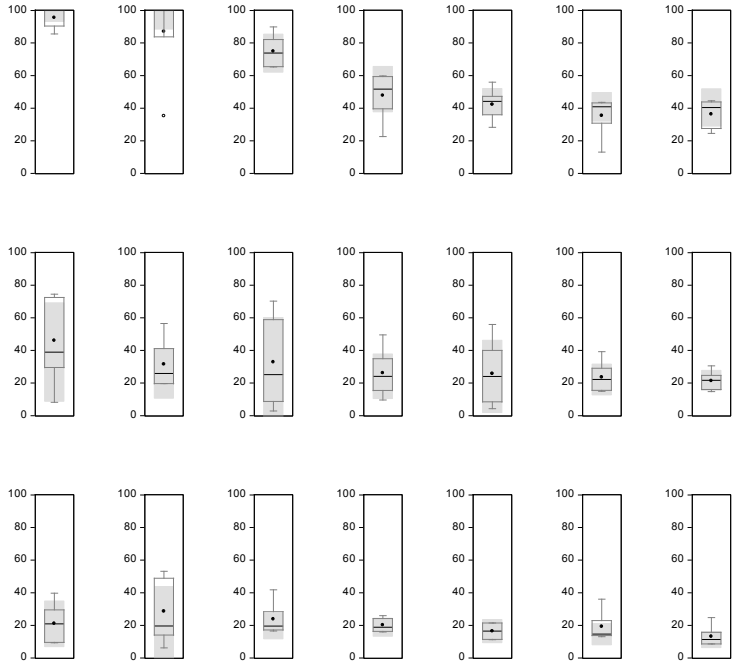

Fig. 7: Box plots of the variable importance measure (VIM), expressed on a scale 1-100, of each pairwise dependence. The VIM are obtained by running the random forest over the single Euro sovereign CDS spreads as dependent variable, and all possible pairwise Kendall's τ (excluding any dependency involving the country of the dependent variable) as covariates. Beginning from the top left and moving towards the right: Italy-France, Spain-Portugal, Spain-Italy, Portugal-Italy, Spain-France, Portugal-France, France-Germany, Greece-Germany, Portugal-Germany, Portugal-Greece, Italy-Germany, Italy-Greece, Ireland-Germany, Spain-Ireland, Ireland-France, Spain-Greece, Spain-Germany, Portugal-Ireland, Greece-France, Italy-Ireland, Ireland-Greece.

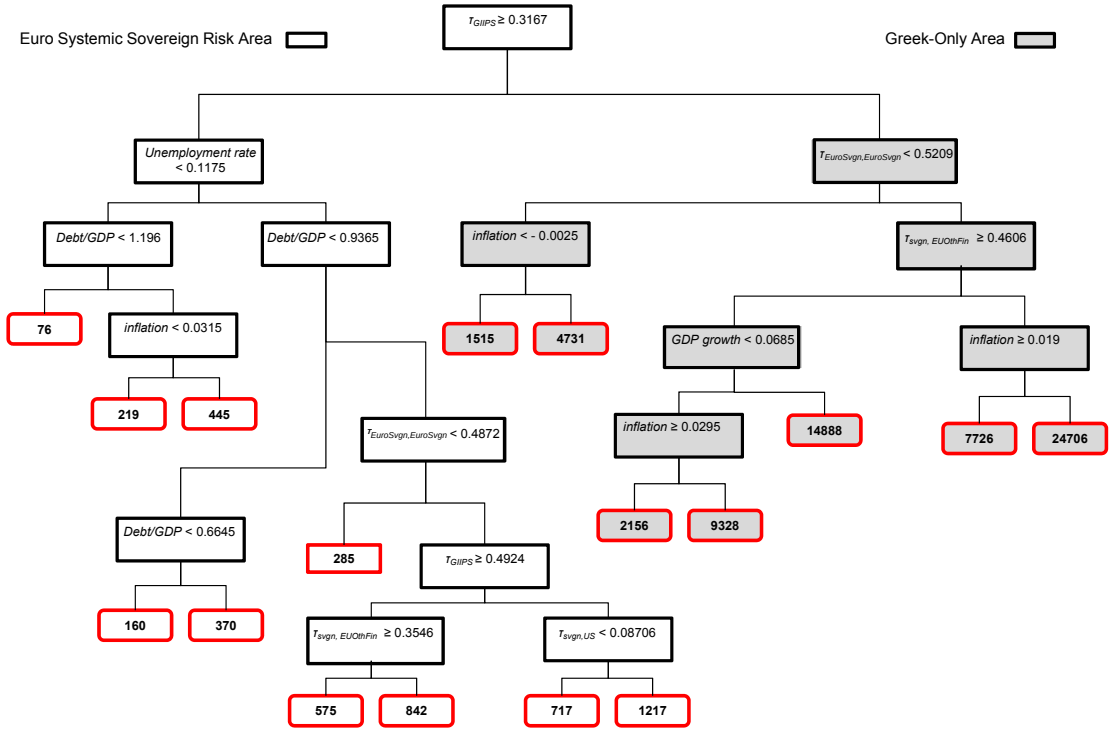

Fig. 8: Sovereign Risk Mapping: Resulting regression tree computed over the entire panel data containing all the Euro sovereign CDS spreads as dependent variable, and fourteen potential leading indicators (eight contagion-based variables and six country-specific fundamentals). Splitting rules are applied in each node until the final one, where the arithmetic average of the CDS spreads (in bps) is reported.

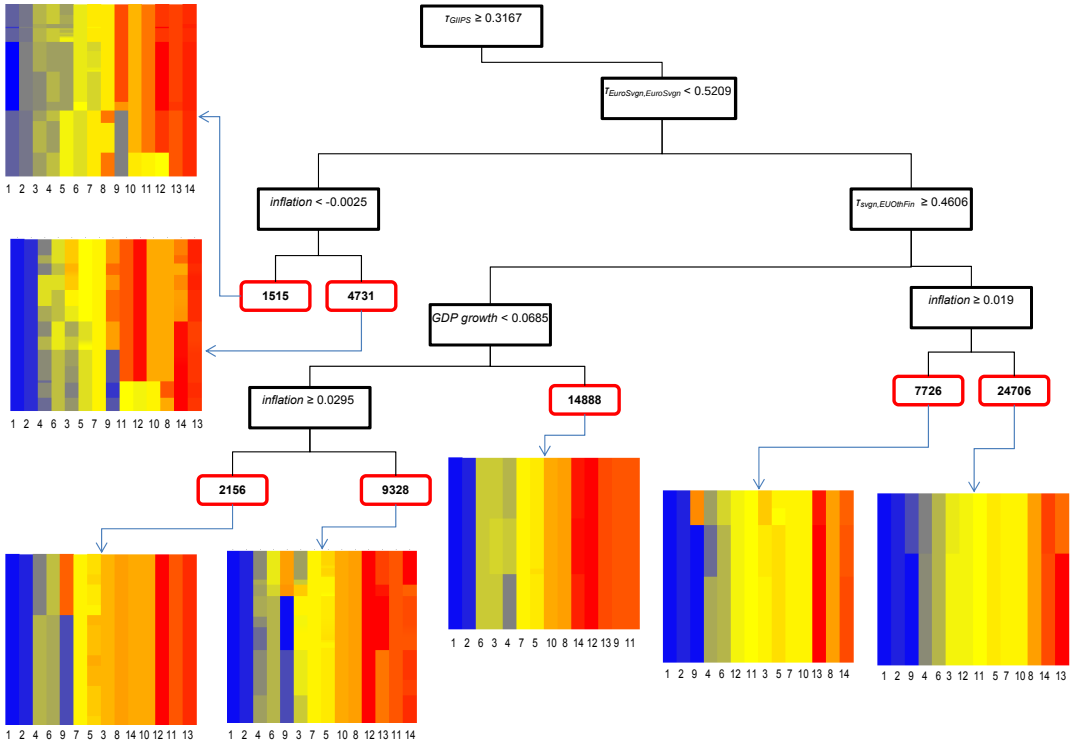

Fig. 9: Greek Only Area Heatmaps. The variables in the heatmaps are the following: 1: τ_{GIIPS}, 2: $\tau_{Fr,Ger}$, 3: *inflation*, 4: *industrial production*, 5: $\tau_{EuroSvgn,EuroSvgn}$, 6: *exports/GDP*, 7: $\tau_{svgn,EUBanks}$, 8: $\tau_{svgn,USBanks}$, 9: *GDP growth*, 10: $\tau_{svgn,US}$, 11: $\tau_{svgn,EUOthFin}$, 12: $\tau_{EuroSvgn,USOthFin}$, 13: *Debt/GDP*, 14: *unemployment rate*. Low values (cold colors) are in blue, high values (hot colors) are in red, while values around the mean (warm colors) are in yellow.

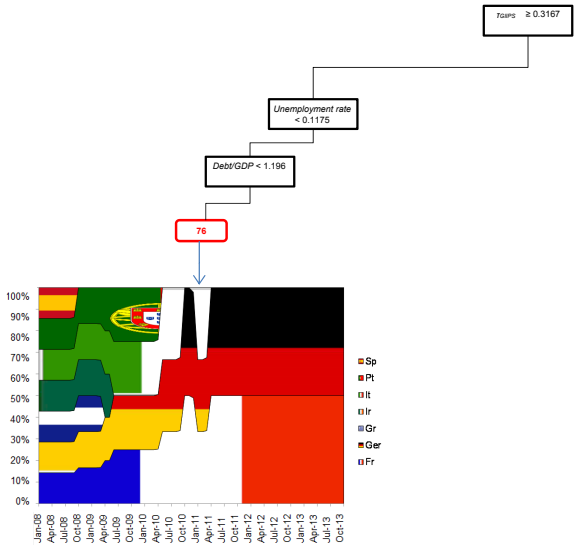

Fig. 10: Safe Zone Country Composition.

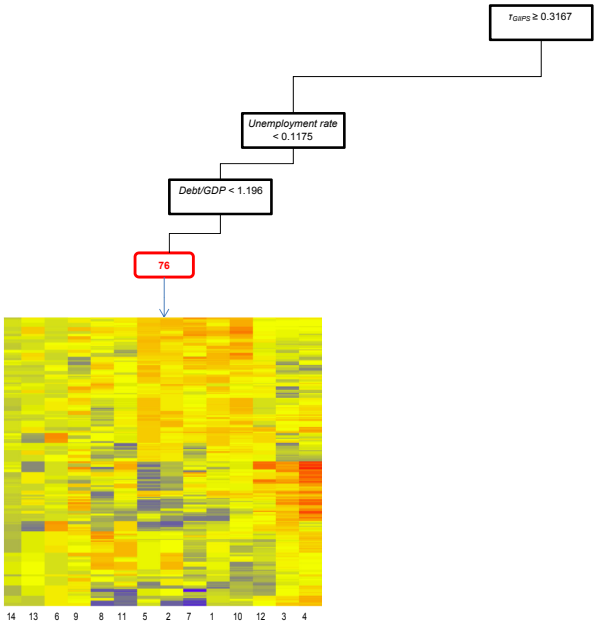

Fig. 11: Safe Zone Heatmap. The variables in the heatmap are the following: 1: τ_{GIIPS}, 2: $\tau_{Fr,Ger}$, 3: *inflation*, 4: *industrial production*, 5: $\tau_{EuroSvgn,EuroSvgn}$, 6: *exports/GDP*, 7: $\tau_{svgn,EUBanks}$, 8: $\tau_{svgn,USBanks}$, 9: *GDP growth*, 10: $\tau_{svgn,US}$, 11: $\tau_{svgn,EUOthFin}$, 12: $\tau_{EuroSvgn,USOthFin}$, 13: *Debt/GDP*, 14:*unemployment rate*. Low values (cold colors) are in blue, high values (hot colors) are in red, while values around the mean (warm colors) are in yellow.

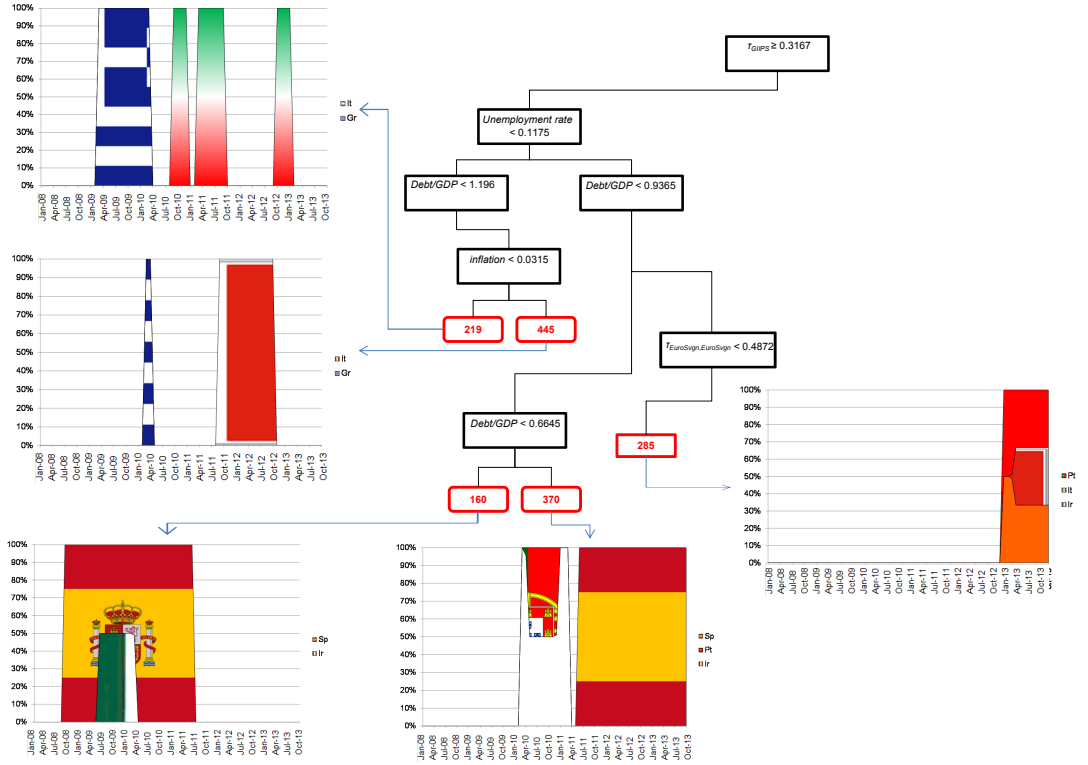

Fig. 12: Risky Zone Country Composition

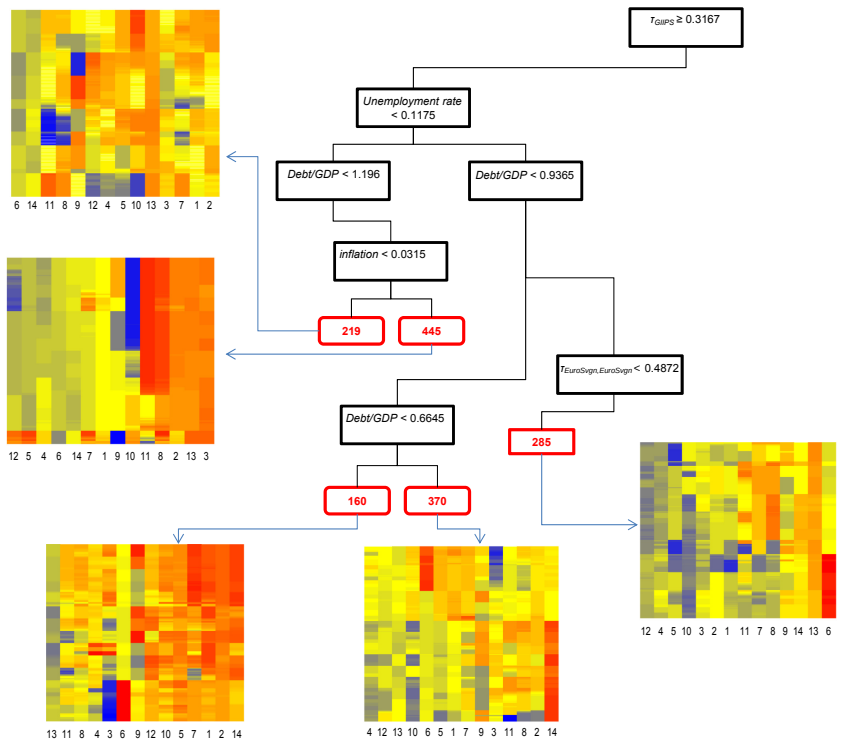

Fig. 13: Risky Zone Heatmaps. The variables in the heatmaps are the following: 1: τ_{GIIPS}, 2: $\tau_{Fr,Ger}$, 3: *inflation*, 4: *industrial production*, 5: $\tau_{EuroSvgn,EuroSvgn}$, 6: *exports/GDP*, 7: $\tau_{svgn,EUBanks}$, 8: $\tau_{svgn,USBanks}$, 9: *GDP growth*, 10: $\tau_{svgn,US}$, 11: $\tau_{svgn,EUOthFin}$, 12: $\tau_{EuroSvgn,USOthFin}$, 13: *Debt/GDP*, 14: *unemployment rate*. Low values (cold colors) are in blue, high values (hot colors) are in red, while values around the mean (warm colors) are in yellow.

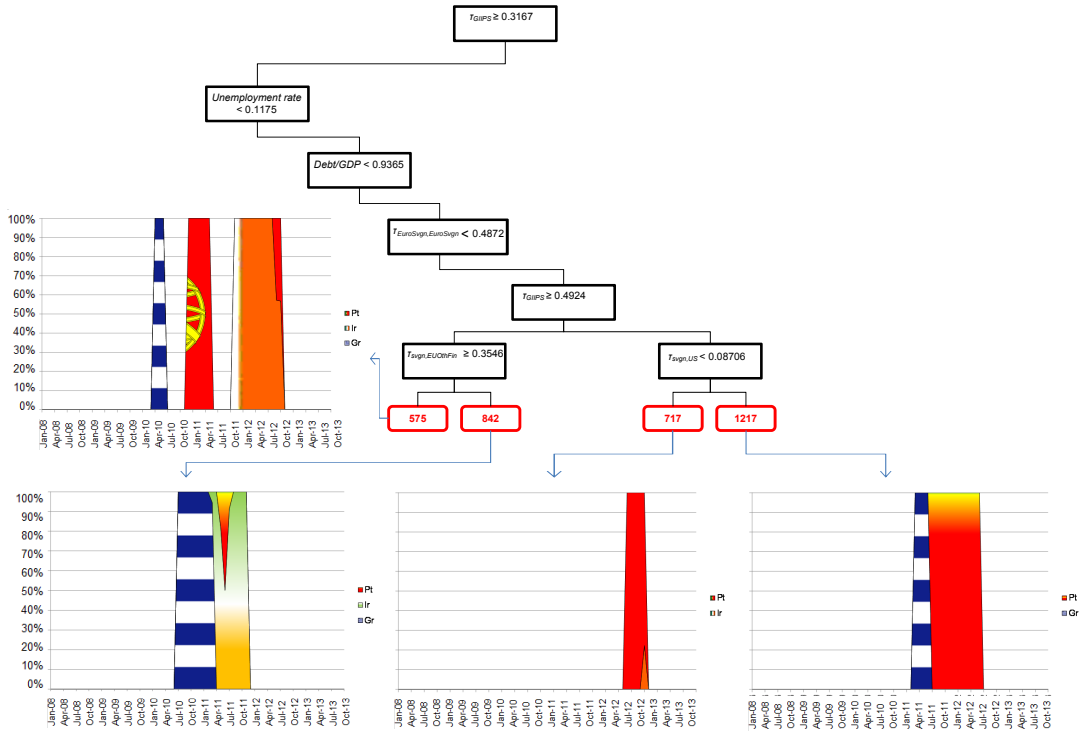

Fig. 14: High Risk Zone Country Composition.

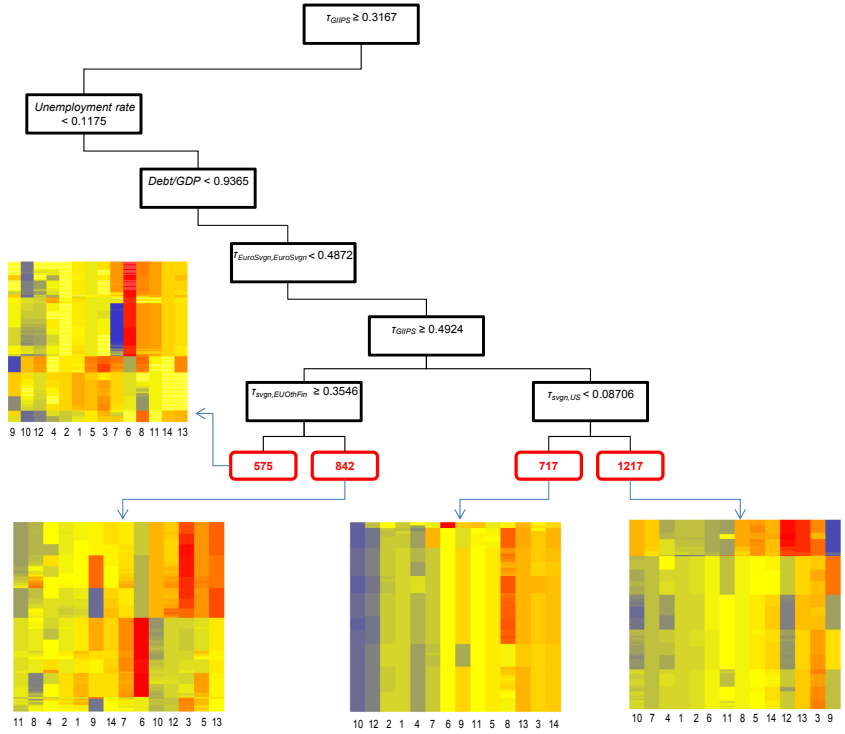

Fig. 15: High Risk Zone Heatmaps. The variables in the heatmaps are the follows: 1: τ_{GIIPS}, 2: $\tau_{Fr,Ger}$, 3: *inflation*, 4: *industrial production*, 5: $\tau_{EuroSvgn,EuroSvgn}$, 6: *exports/GDP*, 7: $\tau_{svgn,EUBanks}$, 8: $\tau_{svgn,USBanks}$, 9: *GDP growth*, 10: $\tau_{svgn,US}$, 11: $\tau_{svgn,EUOthFin}$, 12: $\tau_{EuroSvgn,USOthFin}$, 13: *Debt/GDP*, 14: *unemployment rate*. Low values (cold colors) are in blue, high values (hot colors) are in red, while values around the mean (warm colors) are in yellow.

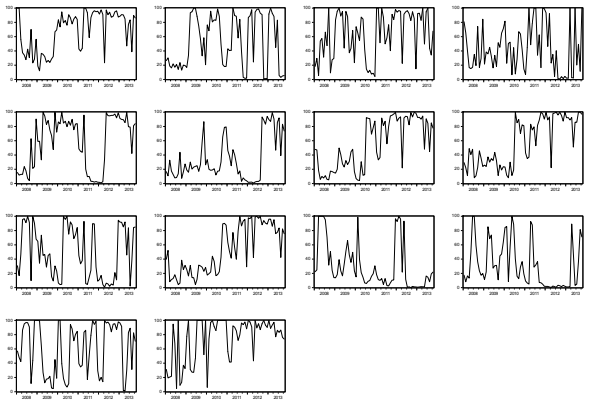

Fig. 16: Time-varying importance of risk indicators: Single time series of all variable importance measure (VIM) obtained by running the random forest over the seven Euro sovereign CDS spreads in monthly frequency, using the fourteen potential leading indicators (eight contagion-based variables and six country-specific fundamentals) as covariates. Beginning from the top left and moving to the right: *Debt/GDP*, *Exports/GDP*, *GDP growth*, *industrial production*, *inflation*, *unemployment rate*, $\tau_{Fr,Ger}$, τ_{GIIPS}, $\tau_{EuroSvgn,EuroSvgn}$, $\tau_{svgn,US}$, $\tau_{svgn,EUBanks}$, $\tau_{svgn,USBanks}$, $\tau_{svgn,EUOthFin}$, $\tau_{EuroSvgn,USOthFin}$.

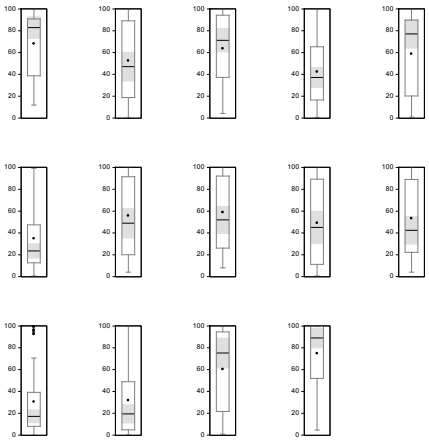

Fig. 17: Risk indicators and their importance: Box plots of the variable importance measure (VIM) obtained as described in Fig.16. Beginning from the top left and moving to the right: *Debt/GDP*, *Exports/GDP*, *GDP growth*, *industrial production*, *inflation*, *unemployment rate*, $\tau_{Fr,Ger}$, τ_{GIIPS}, $\tau_{EuroSvgn,EuroSvgn}$, $\tau_{svgn,US}$, $\tau_{svgn,EUBanks}$, $\tau_{svgn,USBanks}$, $\tau_{svgn,EUOthFin}$, $\tau_{EuroSvgn,USOthFin}$

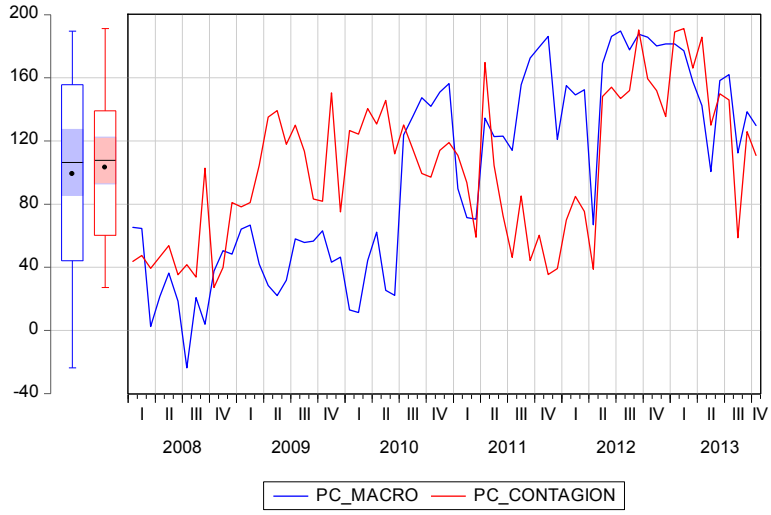

Fig. 18: Time-varying importance of risk indicators: first principal component (pc) extracted from the variable importance measure (VIM) of the first subgroup (pc-contagion) of the eight contagion-based variables, and from the VIM of the second subgroup (pc-macro) of the six country-specific macro fundamentals. Box plots of the two series are on the y-axis.

Online Supplementary Material for "European Sovereign Systemic Risk Zones"

This appendix complements the paper in a number of ways. Section I gives details of the data sources used. Section II describes the family of copulas used in our model framework and Section III analyzes the MCMC technical details. Section IV is a short guide of the codes used to implement the paper and Section V provides an artificial example. In the last section, we provide the results from our MCMC model for the pair of Germany and France.

I. Data sources and ticker identification

Table A.1: CDS data sources and ticker identification

Country	Ticker	Reference Entity	Source
France	FRTR	French Republic	Markit
Germany	DBR	Federal Republic of Germany	Markit
Greece	GREECE	Hellenic Republic	Markit
Ireland	IRELND	Ireland	Markit
Italy	ITALY	Republic of Italy	Markit
Portugal	PORTUG	Portuguese Republic	Markit
Spain	SPAIN	Kingdom of Spain	Markit
US	USGB	United States of America	Markit
EU BANKS 5Y Index	DSEBK5E	DS Europe Banks 5 Year Credit Default Swap Index in euro	Datastream
EU Other Financial 5Y Index	DSEOF5E	DS European Union Other Financial 5 Year Credit Default Swap Index in euro	Datastream
US BANKS 5Y Index	DSNBK5$	DS North America Banks 5 Year Credit Default Swap Index in US dollar	Datastream
US Other Financial 5Y Index	DSNOF5$	DS North America Other Financial 5 Year Credit Default Swap Index in US dollar	Datastream

Table A.2: Macroeconomic data source and ticker identification

Mnemonic	Series Description	Source
prc_hicp_manr	All-items HICP (2005 = 100) - monthly data (annual rate of change)	EUROSTAT
sts_inpr_m	Production in industry - monthly data (2010 = 100)	EUROSTAT
ei_lmhr_m	harmonised unemployment rate (LFS) - monthly data	EUROSTAT
gov_10q_ggdebt	General government gross debt - quarterly data - % on GDP	EUROSTAT
namq_gdp_c	Exports Current prices, Not seasonally adjusted data - Million euro - quarterly data	EUROSTAT
namq_gdp_c	GDP current prices, Not seasonally adjusted data - Million euro - quarterly data	EUROSTAT
namq_gdp_k	GDP volumes, Not seasonally adjusted and adjusted data by working days - Percentage change over previous period - quarterly data	EUROSTAT

II. Copulas

Assume that the financial series X_t and Y_t, $t = 1, \dots T$, are normally distributed with zero means and standard deviations σ^X and σ^Y, and that a bivariate copula function C_t:$[0,1]^2 \to [0,1]$, is chosen to model the joint distribution function of the random variables X and Y, $H(X,Y)$,

$$H(X,Y) = P(\epsilon_t^X \leq x, \epsilon_t^Y \leq y) = C_t(\Phi(\epsilon_t^X), \Phi(\epsilon_t^Y); \theta), \tag{2}$$

where $\epsilon_t^X = X_t/\sigma_X$, $\epsilon_t^Y = Y_t/\sigma_Y$ and Φ denotes the standard Normal distribution function. In our analysis we use the following copulas:

1. *Frank's copula*: $C_\theta^F(u,\nu) = -\frac{1}{\theta}\ln(1 + \frac{(e^{-\theta u}-1)(e^{-\theta\nu}-1)}{e^{-\theta}-1}), \quad \theta \neq 0$

2. *Clayton's copula*: $C_\alpha^C(u,\nu) = [u^{-\alpha} + \nu^{-\alpha} - 1]^{-1/\alpha}, \quad \alpha > 0$

3. *Gumbel's copula*: $C_\beta^G(u,\nu) = exp\{-[(-lnu)^\beta + (-ln\nu)^\beta]^{1/\beta}\}, \quad \beta \geq 1$

where the transformations $\theta = \log\alpha$ and $\theta = \log(\beta - 1)$ allow the parameters of the Clayton's and Gumbel's copulas to lie in the $(-\infty, \infty)$ interval. Frank's copula (Frank (1979)) was chosen for its nice symmetrical properties, whereas Clayton's (Clayton, 1978) and Hougaard - Gumbel's (Gumbel, 1960, Hougaard, 1986) copulas are somehow complementary, since they exhibit opposite upper and lower tail dependence properties.

We generalize (2) by indexing the copula function C by a parameter θ that lies in $(-\infty, \infty)$ (if θ lies in another interval we just perform a simple transformation) and by introducing disjoint sets I_j, $j = 1, \dots, J$, so that

$$C_t(u,v) = \sum_{j=1}^{J} I_j(t) C_{\theta_j}(u_j, v_j) \tag{3}$$

where $[0,T] = \bigcup_j I_j$, $I_j(t) = 1$ if $t \in I_j$, and in each interval I_j the parameter of the copula is θ_j and the corresponding samples x_j and y_j. The copula parameters are also indexed by the interval they belong, indicating that the parameters μ^X, μ^Y, σ^X and σ^Y may be different in each interval I_j. A further generalization of (3) is achieved by employing a collection of copula functions $\{C^i_\theta, i = 1, \ldots, \ell\}$ so that

$$C_t(u,v) = \sum_{j=1}^{J} I_j(t) \sum_{i=1}^{\ell} w_{ij} C^i_{\theta_j}(u_j, v_j) \tag{4}$$

where $C^i_{\theta_j}$ denotes the copula function C^i_θ with $\theta = \theta_j$ and w_{ij} denotes the probability of having the copula i in the interval I_j, so $\sum_{i=1}^{\ell} w_{ij} = 1$ for all j. Thus, our general model (4) allows both the functional form of the copula and the parameters to change within each interval I_j. Note that copula functions model dependence in the tails of the joint distribution, so small sample sizes are not adequate for gathering tail-behavior information and we restrict the length of the each interval to be larger than 15 points.

The dependence between the random variables X and Y is calculated using Kendall's τ, a common alternative to Pearson's correlation measure of association. For completeness we present below the Kendall's τ of the families of copulas used in this paper:

1. *Frank's copula*: $\tau_F = \dfrac{1 - 4(1 - D_1(\theta))}{\theta}, \quad \tau_F \in (-1, 1)$, where $D_k(x)$ is the Debye function, $D_k(x) = \dfrac{k}{x^k} \displaystyle\int_0^x \frac{t^k}{e^t - 1} dt$, $k \in \mathbb{N}$.

2. *Clayton's copula:* $\tau_C = \dfrac{\theta}{\theta + 2}, \quad \tau_C \in [0, 1)$.

3. *Gumbel's copula:* $\tau_G = 1 - \dfrac{1}{\theta}, \quad \tau_G \in [0, 1)$.

III. MCMC Technical Details

III.a. Prior Elicitation

We place non-informative prior model probabilities $f(m) = |M|^{-1}$ and Gamma(1,1) densities for σ^X and σ^Y and for θ a zero-mean Normal prior with variance given by $(\gamma_j - \gamma_{j-1})|H(\widehat{\theta})|^{-1}$, where $H(\widehat{\theta})$ is the Hessian matrix of the likelihood function evaluated at $\widehat{\theta}$.

III.b. Posterior Distribution

Suppose that we have data y that are considered to have been generated by a model m, one of the set M of the competing models. Each model specifies a joint distribution of Y, $f(y|m, \theta_m)$, conditional on the parameter vector θ_m. A Bayesian model determination approach requires the specification of the prior model probability of m, $f(m)$, and conditional prior densities $f(\theta_m|m)$ for each $m \in M$. Then the posterior model probability is given by

$$f(m|y) = \frac{f(m)f(y|m)}{\sum_{m \in M} f(m)f(y|m)}, m \in M \tag{5}$$

where

$$f(y|m) = \int f(y|m, \theta_m) f(\theta_m|m) d\theta_m$$

is the marginal probability of model m. By calculating $f(m|y)$, we have all required information to express our uncertainty about a collection of models M.

III.c. Laplace Approximation

Searching in both model and parameter space is possible via reversible jump algorithm of Green (1995). To facilitate the search, we integrate out the parameter uncertainty

within each model by approximating the marginal likelihood byO

$$\widehat{f}(y|m) = (2\pi)^{d/2}|\widehat{\Sigma}_m|^{1/2} f(y|\widehat{\theta}_m, m) f(\widehat{\theta}_m|m) \tag{6}$$

where $dim(\theta_m) = d$, $\widehat{\theta}_m$ is the maximum likelihood estimate and Σ is the inverse of the Hessian matrix evaluated at $\widehat{\theta}_m$. In our case θ_m is a three-dimensional parameter vector $\theta_m = (\theta, \sigma^X, \sigma^Y)$, so we first appropriately transform each parameter to near-normality and then maximize the likelihood function. By performing this approximation for every model m, we are left with the task to sample in the space of (discrete) density function specified by (5) with $f(y|m)$ replaced by (6).

III.d. MCMC Moves

Assume that the maximum number of thresholds is K. The proposal density $q(m^{'}|m)$, which proposes a new model $m^{'}$, when the current model is m, is constructed as follows. Assume that model m has k thresholds. Then the possible proposal moves are formed as

- *'Birth'*: Propose adding a new threshold.
- *'Death'*: Propose removing one of the k current thresholds if the copula is the same in both sides of the threshold.
- *'Move'*: Propose a reallocation of one of the k current thresholds.
- *'Change'*: Propose a change of a functional form of a copula within two current thresholds.

Denote by b_k,d_k,m_k and c_k the probabilities of 'Birth','Death','Move' and 'Change' moves respectively. Then the proposal densities, for the model m with k thresholds, are formed

as:

$$q(m^{'}|m) = \begin{cases} \dfrac{b_k}{T-k}, & if \quad \text{`}Birth' \\ \dfrac{d_k}{k}, & if \quad \text{`}Death' \\ \dfrac{m_k}{k}, & if \quad \text{`}Move' \\ \dfrac{c_k}{k}, & if \quad \text{`}Change' \end{cases}$$

A sensible choice is b_k=d_k=m_k=c_k=$\frac{1}{4}$, $k = 1, \ldots, K-1$; b_K=d_0=$m_0 = 0$, b_0=c_0=$\frac{1}{2}$, d_K=m_K=c_K=$\frac{1}{3}$. For the 'Move' proposal density we chose a discrete uniform, which takes equidistant values around the current threshold, and we noticed that a length 15 time points, provides a reasonable density spread that achieves a good mixing behavior. We have noticed that some combinations of the four basic moves offer great flexibility in our samplers so the algorithm suggests also the following moves:

- 'Birth-Change': Propose adding a new threshold and changing the copula function in one of the two resulting intervals.

- 'Death-Change': Propose removing one of the current k thresholds when the copula functions are different in each side of the threshold and propose one of the two functions as a candidate for the new interval.

The way we incorporated these extra moves in our sampler is just split all b_k and d_k probabilities to half and thus allow equal proposal probabilities for the 'Birth-Change' and 'Death-Change' moves. The acceptance probability for moving from model m to model $m^{'}$ is given by

$$\alpha = min\{1, \frac{\widehat{f}(y|m^{'})}{\widehat{f}(y|m)} \times R\}$$

where $\widehat{f}$ is the product of all estimated marginal likelihoods in each interval of $[0, T]$ calculated via (6), and R is given by

$$\frac{d_{k+1}}{b_k},\ \frac{b_{k-1}}{d_k},\ 1{,}1$$

for 'Birth', 'Death', 'Move' and 'Change' moves respectively.

We note here that the Metropolis-Hastings moves above resemble the usual reversible jump moves of Denison et al. (2002), but our Laplace approximation (6) essentially removes all the parameter dimension difference between models resulting to a simple acceptance probability without the usual Jacobian terms.

IV. Matlab Code for MCMC

`allclayton.m`: Calculates the MLE estimator of the Clayton copula association parameter and the marginal likelihood of the old and the new model.

`allfrank.m`: Calculates the MLE estimator of the Frank copula association parameter and the marginal likelihood of the old and the new model.

`allgumbel.m`: Calculates the MLE estimator of the Gumbel copula association parameter and the marginal likelihood of the old and the new model.

`allnorm.m`: Calculates the MLE estimators of the marginal densities volatilities.

`bayes_birth_clay.m`: Proposes a new threshold in an interval where the Clayton copula joins the variables.

`bayes_birth_frank.m`: Proposes a new threshold in an interval where the Frank copula joins the variables.

`bayes_birth_gumbel.m`: Proposes a new threshold in an interval where the Gumbel copula joins the variables.

`bayes_birth_only_clay.m`: Proposes a threshold in an interval where no other threshold exists and the Clayton copula joins the variables.

`bayes_birth_only_frank.m`: Proposes a threshold in an interval where no other threshold exists and the Frank copula joins the variables.

`bayes_birth_only_gumbel.m`: Proposes a threshold in an interval where no other threshold exists and the Gumbel copula joins the variables.

`bayes_change.m`: Proposes the change of copula's functional form in a randomly chosen interval.

`bayes_kill_clay.m`: Proposes to kill a threshold in an interval where the Clayton copula joins the variables.

`bayes_kill_frank.m`: Proposes to kill a threshold in an interval where the Frank copula joins the variables.

`bayes_kill_gumbel.m`: Proposes to kill a threshold in an interval where the Gumbel copula joins the variables.

`bayes_kill_max_clay.m`: Proposes to kill the only threshold in an interval where the Clayton copula joins the variables.

`bayes_kill_max_frank.m`: Proposes to kill the only threshold in an interval where the Frank copula joins the variables.

`bayes_kill_max_gumbel.m`: Proposes to kill the only threshold in an interval where the Gumbel copula joins the variables.

`bayes_move_clay.m`: Proposes to move a threshold which belongs in an interval where the Clayton copula joins the variables.

`bayes_move_frank.m`: Proposes to move a threshold which belongs in an interval where the Frank copula joins the variables.

`bayes_move_gumbel.m`: Proposes to move a threshold which belongs in an interval where the Gumbel copula joins the variables.

`laplace.m`: Proposes a new model by choosing among the MCMC moves.

V. Simulation Study

We simulate an example according to the following features:

Subsample	Copula	Marginal probabilities of X and Y variables
1-100	Clayton	N(μ^X=0, $\sigma^X = 0.2$), N(μ^Y=0, $\sigma^Y = 1.5$)
101-400	Frank	N(μ^X=0,$\sigma^X = 2$), N(μ^Y=0, $\sigma^Y = 3$)
401-900	Gumbel	N(μ^X=0, $\sigma^X = 1$), N(μ^Y=0, $\sigma^Y = 1$)
901-1400	Clayton	N(μ^X=0, $\sigma^X = 0.2$), N(μ^Y=0, $\sigma^Y = 1.5$)

We initiated our Markov chain to a model with zero breaks and after a burn-in period of 10×10^4 iterations we obtained our Markov chain output by collecting the next of 20×10^4 samples. In Fig.A.1 - A.4 we can find the posterior probability of the threshold number, the model averaged Kendall's τ, the model averaged volatilities of the marginal distributions of the variables and the posterior probability of the copula model.

VI. MCMC Results

We present the results of the MCMC algorithm for the pair France - Germany. We initiated our Markov chain to a model with zero breaks and after a burn-in period of 10^6 iterations we obtained our Markov chain output by collecting the next of 3×10^5 samples. In Fig.A.5 - A.6 we report the model-averaged posterior mean of Kendall's τ for all pairwise dependencies among the seven Euro sovereign CDS. All the others are available upon request from the authors.

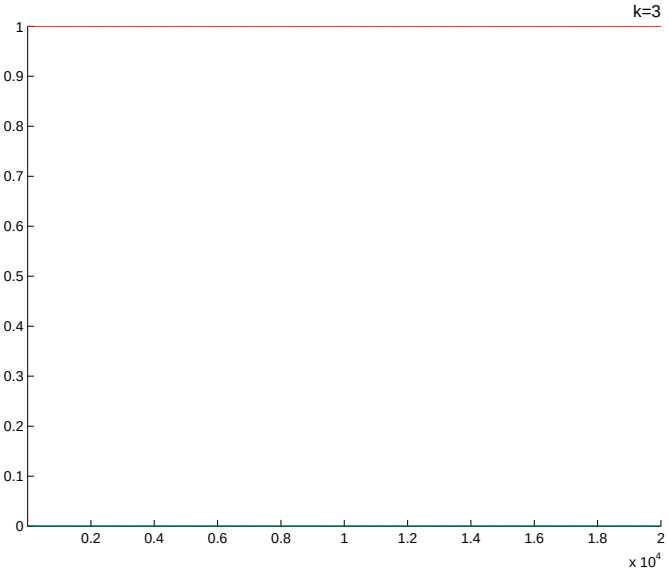

Fig. A.1: Posterior probability of threshold number, k.

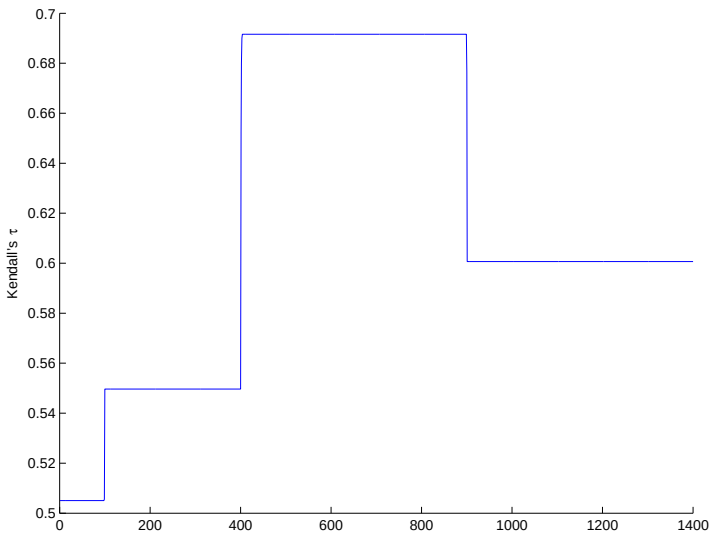

Fig. A.2: Model averaged Kendall's *tau*.

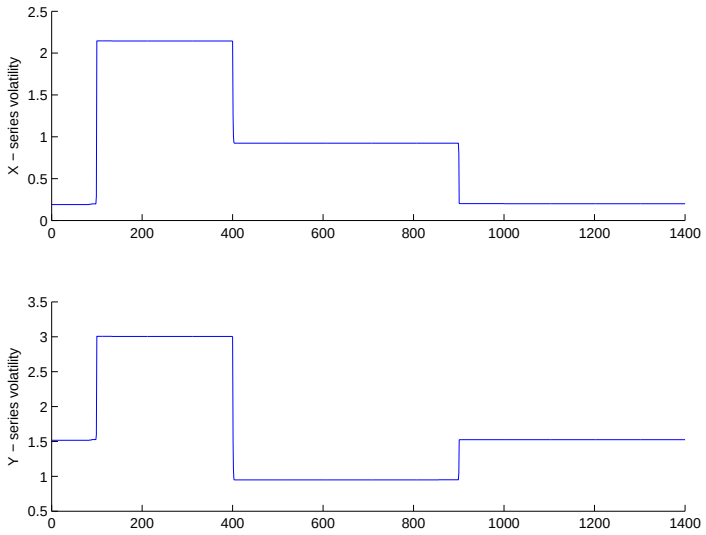

Fig. A.3: Model averaged volatilities of marginal distributions of X and Y variables.

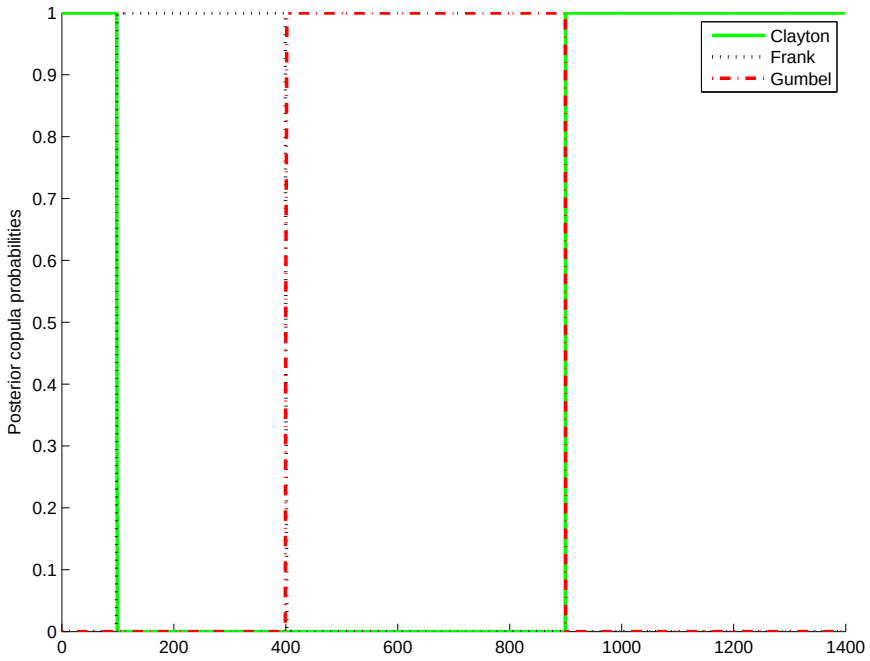

Fig. A.4: Posterior probabilities of copula models.

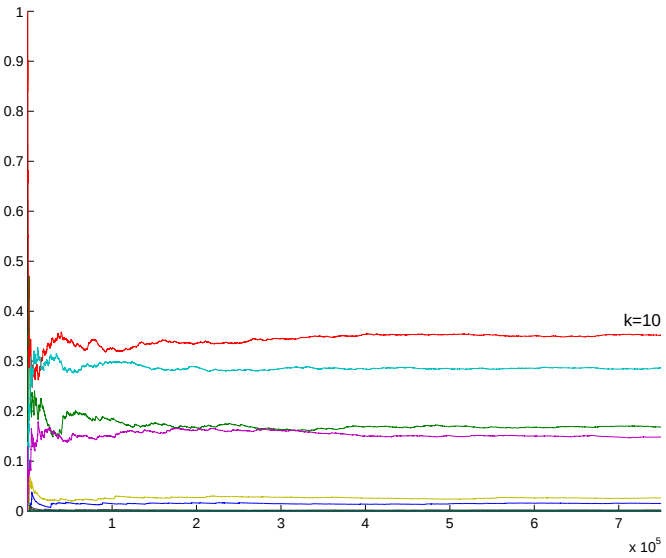

Fig. A.5: Posterior probability of number of threshold, k, for the pair Germany-France.

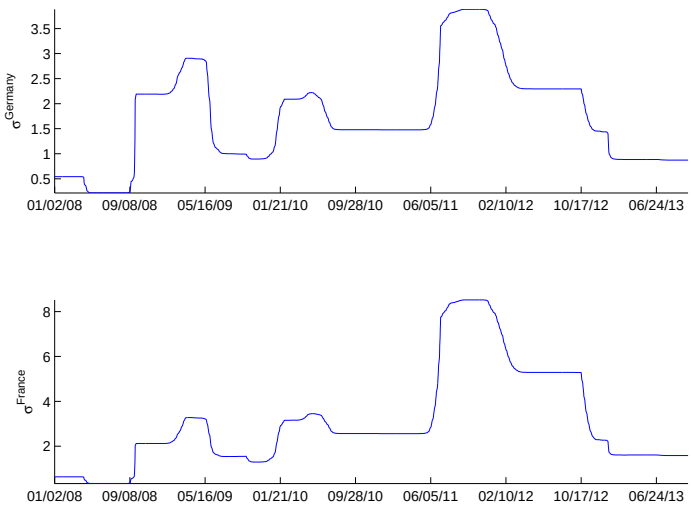

Fig. A.6: Model averaged volatilities of marginal distributions of Germany and France.

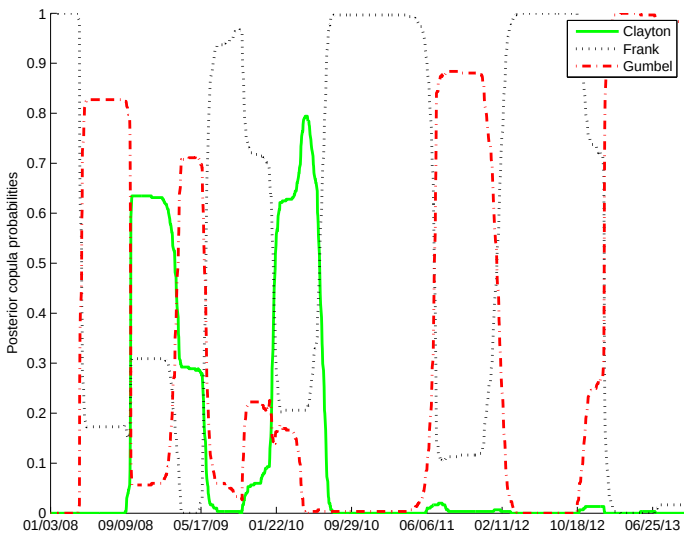

Fig. A.7: Posterior copula probabilities.

References

Clayton, D. G., 1978. A model for association in bivariate life tables and its application in epidemiological studies of familial tendency in chronic disease incidence. Biometrika 65, 141-151.

Denison, D.G. T., Holmes, C. C., Mallick, B. K. and Smith, A.F. M., 2002. *Bayesian Methods for Nonlinear Classification and Regression*, John Willey & Sons.

Frank, M. J., 1979. On the simultaneous associativity of $F(x, y)$ and $x + y - F(x, y)$. Aequationes Mathematicae 19, 194-226.

Green P. J., 1995.) Reversible jump Markov chain Monte Carlo computation and Bayesian model determination. Biometrika 82, 711-732.

Gumbel E. J., 1960. Distributions des valeurs extrêmes en plusiers dimensions. Publ. Inst. Statist., Univ. Paris 9, 171-173.

Hastie, T., Tibshirani, R. and Friedman, J., 2009. The Elements of Statistical Learning: Data Mining, Inference and Prediction, Springer.

Hougaard, P., 1986. A class of multivariate failure time distibutions. Biometrika 73, 671-678.

Kass R. E. and Raftery, A. E., 1995. Bayes Factors. Journal of the American Statistical Association 90, 773-795.